

USE OF STABLE CARBON ISOTOPES TO ASSESS ANAEROBIC AND
AEROBIC METHANE OXIDATION IN HYPERSALINE PONDS

A Thesis
Presented to
The Faculty of the Graduate School
At the University of Missouri-Columbia

In Partial Fulfillment
Of the Requirements for the Degree
Master of Science

By
CLAIRE S. BEAUDOIN
Dr. Cheryl Kelley, Thesis Supervisor
May 2015

The undersigned, appointed by the dean of the Graduate School, have examined the thesis entitled

USE OF STABLE CARBON ISOTOPES TO ASSESS ANAEROBIC AND
AEROBIC METHANE OXIDATION IN HYPERSALINE PONDS

Presented by Claire S. Beaudoin,

A candidate for the degree of Master of Sciences

And hereby certify, that in their opinion, it is worthy of acceptance.

Cheryl Kelley

Kenneth MacLeod

Keith Goyne

To DB.

ACKNOWLEDGEMENTS

I would like to thank Dr. Cheryl Kelley for always lending her expertise and guidance, and for showing me some of the most beautiful places on the Earth to study biogeochemistry. Thanks are also given to Dr. Brad Bebout for his insightfulness, helpful hand in the field, and the use of his laboratory at NASA Ames Research Center. Also to Angela Detweiler, for always helping and providing invaluable support throughout our study. I would also like to thank Dr. Ken MacLeod and Dr. Keith Goynes for reviewing my thesis and providing great feedback. A special thanks goes to Shannon Haynes for her assistance in running some of the samples at the Biogeochemistry Isotope Lab at the University of Missouri. Thanks also to Exportadora de Sal S.A. de C.V. for access to their evaporating ponds in Guerrero Negro, Mexico, and to all of our colleagues in Mexico and Chile, for their hospitality and amazing help in the field. Thank you to my friends and colleagues in the Department of Geological Sciences at the University of Missouri, for being great officemates and friends. Thank you also to NASA Astrobiology Program and the University of Missouri for their financial support.

TABLE OF CONTENTS

Acknowledgements.....	ii
LIST OF TABLES.....	vii
LIST OF FIGURES.....	ix
ABSTRACT.....	xi
Chapter	
1. Introduction.....	1
1.1. Methanogenesis.....	1
1.2. Methane Oxidation.....	1
1.2.1. Anaerobic Oxidation of Methane.....	2
1.2.2. Aerobic Oxidation of Methane.....	3
1.2.3. Methane Oxidation in Hypersaline Environments.....	4
1.3. Stable Carbon Isotopes.....	5
1.4. Previous Work.....	6
1.5. Thesis Overview.....	7
2. Field Sites.....	9
2.1. Sample Collection.....	9
2.2. Guerrero Negro, Baja California Sur, Mexico.....	10
2.3. Atacama Desert, Chile.....	11
2.3.1. Salar de Llamara.....	11
2.3.2. Salar de Atacama.....	12
2.3.3. El Tatio Geyser Field.....	13

3. Methods	14
3.1. Incubations	14
3.1.1. Preparation	14
3.1.2. Analytical Procedure.....	20
3.1.2a. Methane Production Rates	20
3.1.2b. Stable Carbon Isotopes	22
3.2. Dissolved Inorganic Carbon	23
3.2.1. Sample Preparation	23
3.2.2. Analytical Procedure.....	24
3.2.2a. Dissolved Inorganic Carbon Concentrations and $\delta^{13}\text{C}_{\text{DIC}}$ Values	24
3.3. Particulate Organic Matter	25
3.3.1. Sample Preparation	25
3.3.2. Analytical Procedure.....	26
3.4. Ion Concentrations	26
3.4.1. Sample Collection and Preparation.....	26
3.4.2. Analytical Procedure.....	27
3.5. Carbon Mass Balance	27
3.5.1. The Methane Pool.....	27
3.5.2. Carbon Dioxide.....	28
3.6. Data Evaluation.....	29
4. Results	32
4.1. Field Site Data.....	32
4.1.1. Guerrero Negro, Baja California Sur Sites	32

4.1.2. Atacama Desert Sites	32
4.2. Methane Production Rates	33
4.2.1. Unamended Control Incubations	33
4.2.2. $^{13}\text{CH}_4$ -amended Incubations.....	33
4.2.3. Inhibitor Amendments	34
4.3. $\delta^{13}\text{C}_{\text{CH}_4}$ Values	36
4.3.1. Unamended Control $\delta^{13}\text{C}_{\text{CH}_4}$ Values.....	36
4.3.2. Inhibitor $\delta^{13}\text{C}_{\text{CH}_4}$ Values	36
4.4. $\delta^{13}\text{C}_{\text{CO}_2}$ Values	37
4.4.1. Unamended Control $\delta^{13}\text{C}_{\text{CO}_2}$ Values.....	37
4.4.2. $^{13}\text{CH}_4$ -amended $\delta^{13}\text{C}_{\text{CO}_2}$ Values.....	38
4.4.3. Inhibitor Amended $\delta^{13}\text{C}_{\text{CO}_2}$ Values.....	39
4.5. Dissolved Inorganic Carbon	40
4.5.1. Dissolved Inorganic Carbon Concentrations	40
4.5.2. $\delta^{13}\text{C}_{\text{DIC}}$ Values	41
4.5.3. Dissolved Inorganic Carbon Production Rates and Mass Balance	42
4.6. Particulate Organic Matter.....	43
4.6.1. Particulate Organic Carbon Concentrations.....	43
4.6.2. $\delta^{13}\text{C}_{\text{POC}}$ Values.....	44
4.7. Ion Concentrations	44
5. Discussion.....	45
5.1. Site Water Comparisons	45
5.2. Methanogenesis in Hypersaline Ponds	46

5.3. $^{13}\text{CH}_4$ -amended Incubations.....	49
5.3.1. Methane.....	49
5.3.2. Methane Oxidation.....	50
5.4. Inhibitor and $^{13}\text{CH}_4$ + Inhibitor Amendments.....	52
6. Conclusion.....	55
7. References	56
8. Tables.....	60
9. Figures	69

LIST OF TABLES

Tables

- 2.1 Sampling date, water temperatures ($^{\circ}\text{C}$), salinity (ppt), pH, and site descriptions for pond sites in Guerrero Negro, Baja California Sur, Mexico, and the Atacama Desert, Chile. Temperatures measured in surface waters are in bold, otherwise temperatures were taken near the sediment-water interface.....60
- 3.1 Incubation vials prepared in triplicate are denoted by an “X” for sampling locations in Guerrero Negro, Baja California Sur, Mexico, and the Atacama Desert, Chile. Baja 2014 samples denoted with an (*) indicate $^{13}\text{C}_{\text{CH}_4}$ was also added to inhibitor incubations vials in triplicate to create $^{13}\text{C}_{\text{CH}_4}$ +inhibitor treatments.....61
- 4.1 Methane production rates, $\delta^{13}\text{C}_{\text{CH}_4}$ values, and $\delta^{13}\text{C}_{\text{CO}_2}$ values for unamended anaerobic and aerobic incubations, as well as $^{13}\text{C}_{\text{CH}_4}$ -amended incubation vials. Error estimates, in parenthesis, are reported as standard deviations of triplicate samples or half of the range of duplicate samples. The bolded values are statistically different, p values < 0.05, from unamended controls. The aerobic $^{13}\text{C}_{\text{CH}_4}$ -amended Atacama Desert 2013 samples were compared to anaerobic controls.....62
- 4.2 Methane production rates, $\delta^{13}\text{C}_{\text{CH}_4}$ values, and $\delta^{13}\text{C}_{\text{CO}_2}$ values for all Guerrero Negro, Baja 2014 incubations. Error estimates are in parenthesis and reported as standard deviations of triplicate samples or half of the range of duplicate samples. The bolded and italicized values are statistically different, p values < 0.05, from unamended controls, while the bolded $^{13}\text{C}_{\text{CH}_4}$ +Inhibitor values are statistically different from their corresponding inhibitor alone treatment (i.e., $^{13}\text{C}_{\text{CH}_4}$ +BES vs. BES)63
- 4.3 Methane production rates, $\delta^{13}\text{C}_{\text{CH}_4}$ values, and $\delta^{13}\text{C}_{\text{CO}_2}$ values for killed control and $^{13}\text{C}_{\text{CH}_4}$ + killed control incubation vials. Error estimates, in parenthesis, are reported as standard deviations of triplicate samples or half of the range of duplicate samples. The bolded values are statistically different, p values < 0.05, from unamended controls.....64
- 4.4 The $\delta^{13}\text{C}_{\text{POC}}$ values and particulate organic carbon (POC) concentrations for Guerrero Negro, Baja California Sur, Mexico, and Atacama Desert, Chile sites. The $\delta^{13}\text{C}_{\text{DIC}}$ values and dissolved inorganic carbon (DIC) concentrations are from site water collected at each field site. Error estimates are in parenthesis and reported as standard deviations of triplicate samples or half of the range of duplicate samples.....65

4.5 Dissolved inorganic carbon (DIC) concentrations, $\delta^{13}\text{C}_{\text{DIC}}$ values, and DIC production rates for all Guerrero Negro, Baja 2014 incubations. Error estimates are in parenthesis and reported as standard deviations of triplicate samples or half of the range of duplicate samples, except when error was propagated (denoted by an asterisk). Propagated error was reported in place of standard deviations or half ranges only when the calculated error was larger than standard deviations or half ranges. The bolded and italicized values are statistically different, p values < 0.05, from unamended controls, while the bolded $^{13}\text{CH}_4$ +inhibitor values are statistically different from their corresponding inhibitor treatment (i.e., $^{13}\text{CH}_4$ +BES vs. BES).....	69
4.6 Anion concentrations of chloride (Cl^-) and sulfate (SO_4^{2-}) for water samples from Guerrero Negro, Baja California Sur, Mexico and the Atacama Desert, Chile sites. Reported next to approximate concentrations for seawater. Error estimates are in parenthesis and reported as standard deviations of triplicate samples or half of the range of duplicate samples.....	67
4.7 The $\delta^{13}\text{C}_{\text{CO}_2}$ values for unamended control and $^{13}\text{CH}_4$ -amended incubations, $\delta^{13}\text{C}_{\text{DIC}}$ values for sites showing enrichment in $\delta^{13}\text{C}_{\text{CO}_2}$ values between unamended anaerobic controls and $^{13}\text{CH}_4$ -amended incubations. Expected $\delta^{13}\text{C}_{\text{CO}_2}$ values are based on the estimated atom% of CH_4 in $^{13}\text{CH}_4$ -amended incubations, and estimated DIC production rates determined from Area 1 and 9 (Baja 2014) measurements. An estimated and relatively conservative methane oxidation rate of $0.05 \text{ nmol g}^{-1} \text{ d}^{-1}$, based on previously published studies of hypersaline lakes by Iversen et al., 1987, and Joye et al., 1999, was used to calculate expected $\delta^{13}\text{C}_{\text{CO}_2}$ values. Error estimates are in parenthesis and reported as standard deviations of triplicate samples or half of the range of duplicate samples.....	68

LIST OF FIGURES

Figures

2.1 Global locations of study sites Guerrero Negro, Baja California Sur, Mexico, and the Atacama Desert, Chile. (Photo property of Google Earth).....	69
2.2 Guerrero Negro, Baja California Sur, Mexico, sampling locations. Area numbers increase with increasing salinity. (Photo property of Google Earth)	70
2.3 The Atacama Desert, Chile sampling location. Areas include four sites in Salar de Llamara, four in Salar de Atacama, and one site in the El Tatio geyser field. (Photo property of Google Earth).....	71
2.4 Gypsum head from Area 9 of Guerrero Negro, Baja California Sur, Mexico. Colorful laminations of greens and reds distinguish between the different endoevaporite microbial communities. (Photo courtesy of Angela Detweiler).....	72
2.5 Atacama Desert, Chile sampling location. Four site locations at Salar de Llamara (LL 2, 3, 4 and 8), and three at Laguna Cejar (Cejar 1, 2, and 3). (Photo property of Google Earth)	73
2.6 The Atacama Desert, Chile sampling locations. One site location at Laguna Chaxa (CX 1) and one at the El Tatio geyser field. (Photo property of Google Earth).....	74
4.1 Methane production rates for unamended anaerobic and aerobic control incubations vials, and $^{13}\text{CH}_4$ -amended incubation vials. Areas denoted with an asterisk (*) represent Guerrero Negro, Baja 2014 samples.....	75
4.2 The methane production rates for unamended controls, inhibitor, and $^{13}\text{CH}_4$ +inhibitor incubation experiments of Area 1 and Area 9 from Baja (2014). The inhibitor treatments were compared to unamended controls, while the $^{13}\text{CH}_4$ +inhibitor treatments were compared to their corresponding inhibitor alone treatments (i.e., $^{13}\text{CH}_4$ +BES vs. BES).....	76
4.3 The $\delta^{13}\text{C}_{\text{CH}_4}$ values for unamended anaerobic and aerobic control incubations vials. Areas denoted with an asterisk (*) represent Baja 2014 incubations.....	77
4.4 The $\delta^{13}\text{C}_{\text{CO}_2}$ values from unamended controls and $^{13}\text{CH}_4$ -amended incubation vials of Baja (2012 and 2014) and Atacama Desert (2013) sites. Areas denoted with an asterisk (*) represent Baja 2014	

<p>samples. Since aerobic controls were not prepared for the Atacama Desert 2013 study, aerobic $^{13}\text{CH}_4$-amended incubations for Atacama Desert 2013 were compared to anaerobic controls.....</p>	78
<p>4.5 The $\delta^{13}\text{C}_{\text{CO}_2}$ values for unamended controls, inhibitor, and $^{13}\text{CH}_4$+inhibitor incubation experiments of Area 1 and Area 9 from Baja (2014). The inhibitor treatments were compared to unamended controls, while the $^{13}\text{CH}_4$+inhibitor treatments were compared to their corresponding inhibitor alone treatments (i.e., $^{13}\text{CH}_4$+BES vs. BES)</p>	79
<p>4.6 Averaged POC concentrations from Guerrero Negro, Baja California Sur, Mexico, and the Atacama Desert, Chile sites compared to salinity. Areas denoted with an asterisk (*), represent Baja 2014 samples.....</p>	80
<p>4.7 Averaged chloride concentrations (Cl^-) as a function of salinity for water samples collected from Guerrero Negro, Baja California Sur, Mexico, and the Atacama Desert, Chile sites. For reference, estimated chloride concentrations of seawater are plotted (using a chloride seawater value of 560 mM). Areas denoted with an asterisk (*), represent Baja 2014 samples.....</p>	81
<p>4.8 Averaged sulfate (SO_4^{2-}) as a function of salinity for water samples collected from Guerrero Negro, Baja California Sur, Mexico, and the Atacama Desert, Chile sites. For reference, estimated sulfate concentrations of seawater are plotted (using a sulfate seawater value of 29 mM). Areas denoted with an asterisk (*), represent Baja 2014 samples.....</p>	82
<p>5.1 Methane production rates versus concentrations of particulate organic carbon (POC) for all sample sites in Guerrero Negro, Baja California Sur, Mexico, and the Atacama Desert, Chile. Shows methane production rates increase with POC concentrations.....</p>	83

ABSTRACT

Methane oxidation is known to play a significant role in reducing methane (CH_4) concentrations in sediments and water columns in a variety of aqueous environments. In marine systems, for example, it is thought that more than 80% of CH_4 produced is oxidized before reaching the atmosphere. However, under hypersaline conditions, little research has been performed to evaluate methane oxidation. Of the few hypersaline studies undertaken, it is unclear to what extent methane oxidation occurs, although cells of anaerobic methanotrophs have been identified in salinities up to halite saturation.

The focus of this study was to investigate anaerobic and aerobic methane oxidation in organic rich microbial mats and endoevaporite crusts of hypersaline ponds. The two main study areas were the Atacama Desert in Chile and Guerrero Negro in Mexico. To track microbial consumption of CH_4 to carbon dioxide (CO_2), ^{13}C -labeled CH_4 was added to the headspace of incubation vials containing mat and evaporite slurries. After incubating for a period of time between 2 and 90 days, a portion of the biologically produced gaseous headspace was analyzed for $\delta^{13}\text{C}_{\text{CO}_2}$. If methane oxidation was occurring, the measured $\delta^{13}\text{C}_{\text{CO}_2}$ values would be more enriched in ^{13}C compared to control incubations where no $^{13}\text{CH}_4$ was added.

The largest difference between $\delta^{13}\text{C}_{\text{CO}_2}$ values of $^{13}\text{CH}_4$ -containing incubations and corresponding controls was approximately + 4 ‰ to + 7 ‰ in anaerobic treatments of microbial mat and evaporite crusts from Salar de Llamara in Chile. The $\delta^{13}\text{C}_{\text{CO}_2}$ values for the majority of $^{13}\text{CH}_4$ treated incubations, including $^{13}\text{CH}_4$ treatments with added inhibitors, were within ~ 1 ‰ of respective controls. Based on the low amount of ^{13}C -

enrichment in $\delta^{13}\text{C}_{\text{CO}_2}$ values, it appears that little, if any, methane oxidation is occurring in these hypersaline systems.

1. INTRODUCTION

1.1. Methanogenesis

Methanogenic microorganisms in organic-rich natural wetlands are the single largest source of methane emissions to Earth's atmosphere. Microbial activity generates the majority, 80-90 %, of all atmospheric methane, with the remaining 10-20% coming from thermogenic methane and geologic methane from serpentinization reactions (Cicerone and Oremland, 1988, Whiticar, 1999). Methanogens, the obligate anaerobes that produce methane in organic-rich sediments, utilize small fermentation products for energy, metabolizing substrates such as carbon dioxide and hydrogen, acetate, methanol, and other methylated amines for energy (Whiticar, 1999, Killops and Killops, 2005, Reeburgh, 2007). Methanogenesis has been found to occur in a variety of aqueous environments from freshwater sediments and deep-sea hydrothermal vents, and even gypsum crusted hypersaline microbial mats (Oren 1999, Reeburgh 2007).

1.2. Methane Oxidation

Microbial oxidation of methane to carbon dioxide (methanotrophy) can significantly reduce the amount of methane emitted to the atmosphere. For example, on a global scale, 80% of methane rising from the sea floor is oxidized before reaching the atmosphere (Reeburg, 2007). Like methanogenesis, methanotrophy has also been shown to occur in a variety of aqueous environments, such as hypersaline cold seep hydrothermal vents (Maignien 2013), oxic marine water column of southern California Bight (Ward and Kilpatrick 1993), and anoxic freshwater sediments of Lake Washington (Lindstrom and Somers 1984).

In aquatic environments, methanotrophy involves two groups of microorganisms: anaerobic methanotrophic *Archaea* (ANME) and aerobic methanotrophic bacteria (Knittel and Boetius, 2009). The ANMEs are phylogenetically linked to methanogenic *Archaea* and are obligate anaerobes functioning only in the absence of oxygen. The aerobic methanotrophs require oxygen to oxidize methane, limiting their activity to only oxic environments.

1.2.1. *Anaerobic Oxidation of Methane*

Methane oxidation occurring only under anoxic conditions is termed anaerobic oxidation of methane (AOM). In order to oxidize methane, the anaerobic methanotrophic *Archaea* (AMNE) primarily utilize sulfate (SO_4^{2-}) as a final electron acceptor, constructing a symbiotic relationship with sulfate-reducing bacteria (SRB) (Iversen and Jorgensen, 1985, Hoehler et. al., 1994, Boetius et al., 2000). This is a low net energy-yielding metabolic pathway ($\Delta G = -16.9 \text{ kJ}$), which results in the oxidation of methane to bicarbonate (HCO_3^-), reduction of sulfate to hydrogen sulfide (HS^-), and production of water (H_2O) (Equation 1) (Knittel and Boetius, 2009).



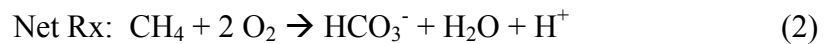
Since sulfate concentrations play a significant role in whether AOM occurs or not, this process is mainly found in anoxic marine environments, as concentrations of sulfate are greater in seawater (29 mM) rather than freshwater ecosystems (100 – 200 μM) (Capone and Keine, 1988). In marine sediments, AOM is typically found within the Sulfate Methane Transition Zone (SMTZ), where methane diffuses upward and sulfate

diffuses downward (Reeburg, 2007, Knittel and Boetius, 2009). The depth of the SMTZ becomes shallower with a greater flux of organic carbon to the sediment (Reeburg, 2007).

1.2.2. Aerobic Oxidation of Methane

Aerobic methanotrophs are obligate aerobes that only function when oxygen is present. These methanotrophs are categorized into two major taxonomic groups and classified by their affinity for methane. Type I methanotrophs have a high affinity for methane, meaning that they are more active in areas where methane concentrations are near atmospheric levels (<2 ppm), while Type II methanotrophs have a low affinity for methane and are dominant in areas where methane concentrations are greater (> 40 ppm) (Chowdhury and Dick, 2013). Both types of aerobic methanotrophs have been found to occupy the same zone in the sediment, with one type usually being more dominant than the other (Hanson and Hanson, 1996).

The aerobic oxidation of methane is a high net energy-yielding pathway ($\Delta G = -813.1$ kJ), resulting in the oxidation of methane by oxygen (O_2) to produce bicarbonate (HCO_3^-), and water (H_2O) and hydrogen (H^+) (Equation 2) (Oren 2001, Oren, 2011).



The highest rates of aerobic methanotrophy occur in soils and sediments with increased rates of methanogenesis and with an extensive vegetative root system capable of supporting oxygen transport to the sediment, such as inundated organic-rich wetland soils, flooded rice fields, and freshwater lakes (Hanson and Hanson, 1996, Chowdhury and Dick, 2013).

1.2.3. Methane Oxidation in Hypersaline Environments

The diversity and growth of microbial communities is limited in hypersaline environments, especially when salt (NaCl) concentrations reach saturation. To survive in hypersaline waters, microbes must adapt to maintain osmotic pressures by either having high intracellular salt concentrations or by allowing organic compatible solutes (like glycine betaine) to balance the osmotic pressure (Oren, 1999). Methanotrophs are known to follow the latter method to maintain osmotic pressure (Oren, 2011). These processes are energetically expensive and, in most cases, occur separately from the biosynthetic and metabolic energy-generating process.

The presence of methane is an essential precursor to whether methanotrophy can/will occur in any environment, including those that are hypersaline. Sources of methane in hypersaline environments can come from geothermal processes, such as the hypersaline sediments at the cold seep mud volcano of Mercator (Maignien et al., 2013), as well as microbial methanogenesis. Methanogens are able to produce methane in salinities up to 250 parts per thousand (ppt) (Oren, 2011). In hypersaline areas having sufficient concentrations of dissolved methane, low levels of methane oxidation (compared to rates of methanogenesis) have also been observed (Joye et al., 1999, Iverson et al., 2007).

1.3. Stable Carbon Isotopes

Stable carbon isotopes can be used to trace the primary carbon source in almost any type of material, including microbial mats, sediment, water, and the atmosphere. Isotope abundance ratios are expressed as per mil (‰) values relative to an internationally accepted standard, Vienna Pee Dee Belemnite (VPDB), using the δ -notation (Equation 3):

$$\delta^{13}\text{C} = [((^{13}\text{C}/^{12}\text{C})_{\text{sample}}) / (^{13}\text{C}/^{12}\text{C})_{\text{standard}} - 1] * 1000 \quad (3)$$

The biological uptake of carbon tends to favor the lighter isotope (^{12}C), leaving the heavier isotope (^{13}C) behind, which causes biological carbon compounds to be relatively enriched in ^{12}C . This isotopic fractionation is due to the slightly faster uptake of ^{12}C in chemical reactions, causing a kinetic isotope effect (Killops and Killops, 2005). For example, when CH_4 is produced, the $\delta^{13}\text{C}_{\text{CH}_4}$ values for biogenic methane range between -110 ‰ and -60 ‰, and the range of thermogenic methane is between -50 ‰ and -20 ‰ (Whiticar, 1999).

In this study, ^{13}C -labeled CH_4 was used as a way to trace the microbial oxidation of methane to carbon dioxide. Since naturally abundant methane and carbon dioxide are produced by microorganisms and depleted in ^{13}C , the ^{13}C of the added methane can be tracked as methanotrophs oxidize the carbon to form CO_2 . By adding $^{13}\text{CH}_4$ (99atom%) to our experiments, any uptake of the heavier isotope by methanotrophs would be observed in the CO_2 pool, causing enrichment in $\delta^{13}\text{C}_{\text{CO}_2}$ values.

1.4. Previous Work

Methane oxidation has been documented in hypersaline environments, occurring in the water column and sediments of Big Soda and Mono Lake, as well as the anoxic sediments of some deep-sea hydrothermal vents (Iversen et al., 1987, Joye et al., 1999, Maignien et al., 2013). One might expect the aerobic oxidation of methane to be more dominant in hypersaline environments, since it has the potential to yield much more energy ($\Delta G = -813.1$ kJ) than AOM ($\Delta G = -16.9$ kJ), and a few Type I (high affinity for methane) species were found to be halotolerant (Heyer et al., 2005, Oren, 2011). However, research has shown that AOM seems to be the dominant process of methane oxidation in hypersaline water columns and sediments, with aerobic oxidation rates occurring at relatively lower rates compared to that of AOM (Iversen et al., 1987, Joye et al., 1999).

At Big Soda Lake, Iversen et al. (1987) showed that methane oxidation was occurring at a relatively low rate of $1.3 \text{ nmol L}^{-1} \text{ d}^{-1}$ in the oxic waters, with methane oxidation rates increasing with depth, and AOM rates of 49 to $85 \text{ nmol L}^{-1} \text{ d}^{-1}$ occurring in the anoxic zone. Joye et al. (1999) measured methane oxidation at Mono Lake using a $^{14}\text{CH}_4$ tracer. They found AOM rates to be 10-fold greater than aerobic rates, with the greatest rate of AOM occurring at 48 nM d^{-1} and the maximum rates of aerobic oxidation at 3.8 mM d^{-1} . In the near-surface sediments of hypersaline hydrothermal vents, Maignien et al. (2013) found AOM activity to be 0.8 and $2 \text{ nmol cm}^{-3} \text{ day}^{-1}$.

1.5. Thesis Overview

Methane oxidation has not yet been studied in the soft microbial mats and evaporite crusts of either Guerrero Negro, Baja California Sur, Mexico, or at the study sites in the Atacama Desert, Chile. Previous research has shown the microbial mat and evaporite crusts at the Guerrero Negro, Baja California Sur salt ponds to contain a range of other microorganisms, including vibrant communities of oxygenic photosynthesizers and heterotrophs (Rothschild et al., 1994, Spear et al., 2003). Methanogenesis has also been observed in the Baja California Sur salt ponds, demonstrating that active methanogenic communities can live within a large range of salinities (Bebout et al., 2004). These studies helped spur the possibility that methanotrophs may also inhabit the hypersaline microbial mats and evaporite crusts in Guerrero Negro and the Atacama Desert.

The objective of this study is to test the hypothesis that methane oxidation is occurring in hypersaline areas where methanogenesis has been shown to occur. This research not only expands on the scope of the few studies that have investigated methane oxidation in hypersaline environments (Iversen et al., 1987, Joye et al., 1999, Maignien et al., 2013), but can also lend itself to understanding the potential influence methane oxidation could have on stable carbon isotopes produced by microbial communities within hypersaline areas.

To implement this study, methane production rates were measured from (anaerobic and aerobic) control and experimental incubation vials of soft microbial mat and evaporite crust from hypersaline areas. In experimental vials, $^{13}\text{CH}_4$ -amendments were used to trace the oxidation of the methane into the CO_2 pool. Inhibitors were used to

evaluate how the oxidation of methane would affect the CO₂ pool under different substrate conditions. Statistical increases in $\delta^{13}\text{C}_{\text{CO}_2}$ values between unamended controls and ¹³CH₄-amended incubation vials were used to determine the possible occurrence of methane oxidation.

For Baja 2014 sample incubations, the dissolved inorganic carbon (DIC) concentrations and $\delta^{13}\text{C}_{\text{DIC}}$ values of the incubation water within the vials were measured for a comparison of internal biogeochemical conditions to data collected in the field. This data was also used to estimate DIC production rates and to calculate the expected $\delta^{13}\text{C}_{\text{CO}_2}$ values if methane oxidation rates were to occur at similar rates observed in other hypersaline areas. Supplementary data was also collected from the field sites. These data include particulate organic carbon (POC) concentration and $\delta^{13}\text{C}_{\text{POC}}$ values, water temperature, salinities, sulfate and chloride concentrations, and DIC concentrations and $\delta^{13}\text{C}_{\text{DIC}}$ values.

2. FIELD SITES

The hypersaline field sites used in this study were located in Guerrero Negro, Baja California Sur, Mexico, and the Atacama Desert, Chile (Figure 2.1-2.3). Sampling locations and site descriptions are listed in Table 2.1. The sampling sites in Mexico and Chile were selected based on previously published data supporting the occurrence of biologically produced methane within these hypersaline ponds (Kelley et al., 2012, Kelley et al., 2014). At all sites, site water and microbial mat or crust was collected to determine methane production rates and stable carbon isotopes.

2.1. Sample Collection

Microbial mat or evaporite crust and overlying pond water was collected from several ponds throughout the Atacama Desert, Chile in May 2013, and from Guerrero Negro, Baja California Sur, Mexico in November 2012 and March 2014. In the field, the water temperature near the sediment water interface was measured using a thermometer, and at sites with a noticeable difference in temperature between the surface and bottom waters, the surface water temperatures were also measured. The only site location with noticeably different water temperatures, where surface water temperature was measured, was at Salar de Llamara. At the time of collection (or shortly after collection), the salinity of the overlying pond water was measured using a hand-held refractometer.

The site locations were chosen to include a variety of microbial mat and evaporate crusts from a wide range of salinities, and to avoid areas disturbed by local fauna and tourists. A metal spatula was used to cut the soft mats out of their natural environment and a hammer and metal spike were used to break apart evaporite crust materials. Mats

and crusts were stored in airtight Ziploc bags. Site water samples, and microbial mat and evaporite crust samples were refrigerated. This was done to slow down microbial activity until experiments could be prepared in the laboratory.

2.2. Guerrero Negro, Baja California Sur, Mexico

Located on the west coast of the Baja Peninsula, Baja California Sur, Mexico, the hypersaline ponds used in this study are owned by the salt production company, Exportadora de Sal S.A. de C.V. In order to harvest salt, seawater from the Laguna Ojo de Liebre is pumped into a retention area made up of several interconnected ponds. As water gravitationally flows from pond to pond, the water increasingly becomes more saturated with sodium chloride (NaCl) due to the natural concentration processes of solar- and wind-induced evaporation. In the final stage, ponds supersaturated in NaCl are allowed to completely evaporate to form salt crystals for harvesting. The designated numbers for each pond (Area 1, Area 2, etc.) reflect increases in salinity, with crystallization of gypsum (CaSO_4) and halite (NaCl) occurring in the higher numbered ponds, beginning at salinities around 130 ppt (Shumilin et al., 2002).

Samples for this study were collected from Area 1, 9, and 10 (Figure 2.2). Study sites were selected based on previously collected site bubbles, which contained relatively high concentrations of methane (up to 45%) and mat incubations that show high methane concentrations and production rates for these areas (Kelley et al., 2012, Tazaz et al., 2013). Samples of Area 1 microbial mats were organic-rich, and approximately 2-3 cm thick. The Area 9 evaporite crust, which is made of gypsum, used for this study contained several layers of green and red microbial communities beneath the surface

(Figure 2.4). The gypsum crusts collected at Area 10 were similar to Area 9. In 2012, the sediment directly below the microbial mats and evaporite crusts of Areas 1 (Area 1-Deep) and 10 (Area 10-Deep) were also collected.

2.3. Atacama Desert, Chile

The Atacama Desert, known as the oldest and driest desert on Earth (McKay et al., 2003), is located in northern Chile along a plateau west of the Andes Mountains. Due to its arid climate and low annual precipitation, totaling only a few millimeters, the extreme measures under which life survives in the Atacama Desert has been used as an analogue for reconstructing past environmental settings on Earth and other planetary bodies, such as Mars (McKay et al., 2003, Smith et al., 2014). Many scientists have become particularly interested in hypersaline water bodies in the Atacama Desert that have become hosts to a variety of extreme microorganisms (Demergasso et al., 2010).

For this study, several locations were sampled within the Atacama Desert, Chile, including ponds in Salar de Llamara, Salar de Atacama, and the El Tatio geyser field (Figures 2.3 and 2.5). These sites are described in more detail below.

2.3.1. Salar de Llamara

Several small hypersaline evaporite ponds that collectively make up Salar de Llamara are located in the central depression west of the Andes Mountains. The elevation at Salar de Llamara is approximately 750 m above sea level. The groundwater entering the central depression, located between the Coastal Range and the Andes, is likely to react with the volcanic bedrock underlying the basin, acquiring a variety of dissolved ions

before entering the salar (Pueyo et al., 2001). Site water and microbial mats and crusts were collected from four sites (LL 2 - 4, and 8). See Figure 2.5 for relative site locations.

Samples collected from sites LL 2 and LL 3 were both hard gypsum crusts taken from the bottom of a large shallow pool, with site LL 3 being centrally located within the pool compared to site LL 2, which was sampled near the southern edge. The microbial mats collected from sites LL 4 and LL 8 were from smaller pools where the mat materials were soft and contained purple coloration throughout.

2.3.2. Salar de Atacama

Salar de Atacama is located in the Pre- Andean depression at an elevation of approximately 2300 m above sea level. Known as the largest salar in the Atacama Desert, the system is about 2900 km² and contains many interior ponds (Demergasso et al., 2004). Two evaporating ponds were sampled in the Salar de Atacama, Laguna Cejar (Cejar 1, 2 and 3) and Laguna Chaxa (CX 1).

Three sites were sampled at Laguna Cejar, the first along the organic-rich edge of the large central pool (Cejar 1), the second from the shallow organic-rich channel-like feature closer to the center (Cejar 2), and the third from the shallow edge of the deep gypsum crusted pool at the center (Cejar 3). The microbial mat sampled at Laguna Chaxa (CX 1) appeared organic-rich and was located near the end of the walking path where the mats were less disturbed by tourists. See Figure 2.5 and Figure 2.6 for relative site locations.

The soft microbial mats collected at Cejar 1 had a thin white-pink exterior covering a dark green sediment, while Cejar 2 mats smelled sulfidic and consisted of colorful wavy-laminated layers. The hard gypsum crusts used from Cejar 3 contained

layers of green and red microbial communities beneath the surface. The soft microbial mats collected at CX 1 had a thin layer of greenish-pink crust with layers of green and purple communities underneath.

2.3.3. El Tatio Geysir Field

Covering approximately 10 km², the El Tatio geysir field is the largest geothermal area in the southern hemisphere (Fernandez-Turiel et al., 2005). At an elevation of about 4200 m above sea level, the site sampled (ET 2) in the geysir field marks the highest elevation sampled in our study. The water in the hot springs originates from meteoric rain and snow coming off the Andes, infiltrating the bedrock and getting heated by the residual heat caused by local volcanism (Jones and Renault, 1997). At this elevation, the boiling of water occurs at a temperature of 86° C. The hot springs at El Tatio host a number of extremophiles, including those that can tolerate high levels of ultraviolet radiation due to the low latitude and high elevation, as well as those that can withstand extreme temperatures (Dunckel et al., 2009). The sediment collected at ET 2 was from a small, cool freshwater pool and appeared organic-rich.

3. METHODS

3.1. Incubations

The incubation treatments prepared for each site are listed in Table 3.1. The treatments used in this study include unamended controls (site microbial mat/crust and water only), treatments with added 99 atom% labeled-methane ($^{13}\text{CH}_4$), killed control treatments with added paraformaldehyde, and inhibitor treatments including 2-bromoethanesulfonate (BES), sodium molybdate, and picolinic acid. The incubation vials were also set up under anoxic and oxic conditions.

3.1.1. Preparation

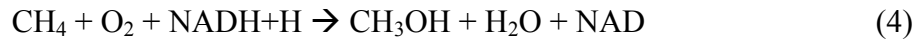
Incubations were set up to determine methane production rates, and evolved $\delta^{13}\text{C}_{\text{CO}_2}$ and $\delta^{13}\text{C}_{\text{CH}_4}$ values under anaerobic and aerobic conditions for study sites in Guerrero Negro, Baja California Sur, Mexico (Area 1, 9, and 10) and the Atacama Desert, Chile (LL 2,3,4, and 8, Cejar 1,2, and 3, CX 1, and ET 2). All of the incubations were prepared at NASA Ames Research Center, except for the Baja 2012 incubations, which were prepared in Guerrero Negro, Mexico. In all cases, incubation vials were set up in triplicate in pre-weighed 38 mL serum bottles using 10 mL of site water and between 8 g and 32 g of homogenized microbial mat or evaporite crust. The mass of the homogenized site material added to incubation vials was determined by organic matter content, with less material needed of the organic-rich soft microbial mats compared to the gypsum evaporite crust. For anaerobic experiments, site water was bubbled with N_2 gas for at least 5 minutes (before adding to serum vials) to remove dissolved O_2 from the water. Site water was not bubbled for aerobic experiments. Unamended (no ^{13}C added) controls consisted of only site water and microbial mat or crust slurry.

To track the oxidation of methane in the incubation vials, 25 μL of 99 atom% ^{13}C -labeled methane ($^{13}\text{CH}_4$) gas was injected into incubation vials. Since biologically produced methane and carbon dioxide are naturally abundant in ^{12}C , adding $^{13}\text{CH}_4$ to the headspace allowed us to observe the oxidation of methane as positive changes in $\delta^{13}\text{C}_{\text{CO}_2}$ values.

Inhibitors included in the Baja 2014 incubations were added to determine how methane oxidation rates in hypersaline microbial mat and crusts would change $\delta^{13}\text{C}_{\text{CO}_2}$ values. To observe methane oxidation under different substrate conditions, three inhibitor amendments/treatments were used: sodium molybdate (Moly) was used to inhibit sulfate reduction, picolinic acid was used to inhibit aerobic methane oxidation, and 2-bromoethanesulfonate (BES) was used to inhibit methanogenesis.

The anaerobic oxidation of methane (AOM) is known to occur as a consortium between sulfate-reducing bacteria (SRB) and methanotrophic *Achaea*. Sodium molybdate was added to incubation vials to determine how the inhibition of SRB would affect this relationship. As an analogue for sulfate (SO_4^{2-}), sodium molybdate inhibits the anaerobic use of sulfate by SRB. The molybdate anion replaces the sulfate ion, blocking the formation of APS (adenosine-5'-phosphosulfate) by attaching itself to form the unstable analogue of APMo (Oremland and Capone, 1988). In most cases, this process stops the reduction of sulfate and stimulates the production of methane (Capone and Kiene, 1988). Molybdate was added to a final concentration matching previously measured in-situ SO_4^{2-} concentrations of the site water at each location. Final concentrations of molybdate were 40 mM at Area 1, and 126 mM at Area 9.

Picolinic acid was added to aerobic incubations to inhibit aerobic bacterial methane oxidation, in order to determine if and at what rate aerobic methane oxidation occurs at these hypersaline sites. The first step in methane oxidation is the oxidation of methane to methanol (CH₃OH) and water (H₂O) (Equation 4) (Bernard and Knowles, 1989):



where oxygen (O₂), and NADH+H and NAD⁺ are, respectively, the reduced and oxidized forms of nicotinamide adenine dinucleotide (which is used in many cellular pathways to form energy). Picolinic acid inhibits the enzyme catalyst for this reaction, methane monooxygenase (MMO), blocking the oxidation of methane (Bodelier and Frenzel, 1999). It is important to note that picolinic acid is not a specific inhibitor to methane oxidation, as the structure of MMO is homologous to the structure of ammonia monooxygenase found in ammonia (NH₄⁺)-oxidizing bacteria, causing picolinic acid to inhibit the oxidation of ammonia (Bernard and Knowles, 1989). Previous studies reported the inhibition of soil methane oxidation when using picolinic acid concentrations of 500 μM, but when using picolinic acid concentrations < 1 mM, aerobic methanotrophs began oxidizing methane again after an incubation period of 20 hours (Bernard and Knowles, 1989, Bodelier and Frenzel, 1999). It was also shown that picolinic acid concentrations of 2 mM did not inhibit the production of nitrate by ammonia oxidizing bacteria (Bernard and Knowles, 1989). Therefore, a final concentration of 1 mM of picolinic acid was added to incubation vials to inhibit aerobic methane oxidation.

BES was used to observe how the inhibition of methanogenesis would affect $\delta^{13}\text{C}_{\text{CO}_2}$ values and the overall oxidation of methane in hypersaline microbial mat and crusts. BES is a known analogue of mercaptoethanesulfonic acid, coenzyme M (CoM), which is found only in methanogenic bacteria (Capone and Keine, 1988). This makes BES a specific inhibitor of methanogenesis. The terminal methylation reaction from CoM to methyl-CoM reductase enzyme complex occurs through a methyltransferase reaction (Oremland and Capone, 1988). By inhibiting CoM, the methyltransferase reaction cannot occur, stopping the reduction of methyl-CoM and the ultimate release of methane. The final concentration of BES added to incubation vials was 100 mM. This was to ensure the complete inhibition of methanogenesis, as previous research suggests concentrations of 100 mM BES are necessary for complete inhibition (King, 1984, Oremland and Capone, 1988).

Only one inhibitor was added per vial. The added volumes of molybdate were determined by the naturally occurring concentration of sulfate within each hypersaline environment, and the added volumes of picolinic acid and BES were determined by observations made in previous inhibitor research (Oremland and Capone, 1988, Bodelier and Frenzel, 1999). High concentrations of sodium molybdate (40 mM to 126 mM) and BES (100 mM) were necessary to inhibit the reduction of sulfate and methanogenesis, respectively; therefore the desired concentrations of each inhibitor were made in 10 mL of site water and added directly to the serum vials. The necessary concentration of picolinic acid (1 mM) was much smaller, requiring a small amount (200 μL) of a highly concentrated stock solution (50 mM) to be added directly to the serum vials along with the 10 mL of site water. Inhibitor solutions for aerobic experiments were not bubbled,

while solutions made for anaerobic experiments were bubbled using N₂ gas before adding to serum vials. Incubation vials were also prepared to include an inhibitor + ¹³C-labeled methane gas (¹³CH₄). The types of inhibitor incubations prepared are summarized in Table 3.1.

Data collected from ¹³CH₄-treated incubation vials, including measured δ¹³C_{CO₂} values, were compared to the data collected from unamended controls, while inhibitor + ¹³CH₄ treated incubations were compared to incubation vials containing the corresponding inhibitor alone treatments (i.e., incubation vials with added inhibitor were used as controls for inhibitor + ¹³CH₄ treatments). Inhibitor + ¹³CH₄-treatments were prepared in order to trace the oxidation of the ¹³C of the labeled methane under different substrate conditions.

Killed control treatments were prepared to make sure the emissions from microbial mat and crust slurries were biogenic. The killed control and ¹³CH₄ + Killed-control incubations in the Baja 2014 study also serve a second purpose. This was to show that any differences observed in δ¹³C_{CO₂} values between controls and ¹³CH₄-amendments were most likely due to the metabolic use of the ¹³CH₄, and not an exchange of carbon atoms between ¹³CH₄ and carbon dioxide (CO₂) in the incubation headspace. Killed control vials were prepared using 2 mL to 2.5 mL of 20% paraformaldehyde and 7.5 mL to 8 mL of site water for a final concentration of 4%-5% paraformaldehyde solution. Although the use of a 4% paraformaldehyde solution in the Baja 2012 study was effective, paraformaldehyde concentrations were increased to 5% for the Atacama Desert 2013 and Baja 2014 studies. Killed controls were set up at all locations, except for Areas 1, 1-Deep, and 9, in the Baja 2012 study. Killed controls were not set up at these

locations in 2012, as the emissions from these sites were already recognized to be of biogenic origin (Rothschild et al., 1994, Spear et al., 2003).

After all materials were added, serum vials were capped with butyl rubber stoppers and aluminum crimps. With the exception of the killed control vials, the headspace in the anaerobic incubations vials were flushed with N₂ gas for 5 minutes to remove any O₂ gas. Aerobic incubations either remained unaltered (Atacama Desert 2013) or were injected with 2 mL of 99% O₂ gas (Baja 2014). The addition of O₂ gas was made to prevent the incubations from becoming anoxic, which was likely the case for some of the previously set up experiments (Atacama Desert 2013) containing a high percentage of organic material.

The sets of incubations prepared at each site varied and are listed in Table 3.1. The incubations set up from the Baja sites in 2012 focused specifically on anaerobic methane oxidation at 5 site locations, all together totaling 36 incubations vials. For each site location, incubations included 1 set of unamended controls, 1 with added ¹³CH₄, and two site locations also included 1 set of killed control vials (all prepared in triplicate). The Atacama Desert 2013 incubations were set up to observe both anaerobic and aerobic methane oxidation at 9 site locations, having an overall total of 108 incubations vials. At each location in the Atacama Desert, 1 set of unamended controls, 2 sets with added ¹³CH₄, and 1 set of killed control vials were prepared in triplicate. All anaerobic vials (and aerobic vials from Atacama Desert 2013) were stored in the dark at room temperature, and upside down with the slurry covering the stopper. This was done to avoid the exchange of gases through the puncture holes in the stopper. The Baja 2014 experiments included both anaerobic and aerobic incubations for 2 site locations, totaling

84 incubation vials. At each site, 2 set of unamended controls, 2 sets with added $^{13}\text{CH}_4$, 4 sets of inhibitor treatments, 4 sets of an inhibitor + $^{13}\text{CH}_4$, 1 set of killed controls, and 1 set of killed controls + $^{13}\text{CH}_4$ treatments were all prepared in triplicate. The aerobic treatments were stored at room temperature, upside down in an open box on the laboratory bench top. Storing the aerobic incubations on the lab bench increased the availability of light during the day, which helped to maintain photosynthetic pathways and the overall presence of oxygen in the headspace.

3.1.2. Analytical Procedure

3.1.2a. Methane Production Rates

Methane production rates were calculated from methane concentration measurements taken at known time intervals from the headspace of incubation vials. Before taking methane concentration measurements, vials were shaken for about 2 minutes to drive any dissolved or trapped methane from the slurry into the headspace. Concentrations were measured for all sites using a Shimadzu gas chromatograph (GC-14A) at NASA Ames Research Center, operating with a flame ionization detector and a Porapak Q column. The first concentration measurements were taken within 24 to 48 hours of incubation start time, with an effort made to take first measurements as soon as possible. Depending on the methane production rate occurring in each set of vials, incubation times varied along with the frequency of methane concentration measurements. For example, incubations producing methane at higher rates (i.e., Cejar 1) incubated for less time and were measured more frequently, while sites producing methane at low rates (i.e., LL 4) were incubated for a longer time interval and measured less frequently. Methane was measured until concentrations reached approximately 1000

ppm, at which point samples were frozen (still inverted) to halt biological activity until stable carbon isotope analysis could be measured at the University of Missouri.

Incubation times lasted from 2 days (CX 1) to 90 days (Area 10).

A linear regression analysis was used to fit to measured methane concentrations over time in order to calculate production rates for each incubation vial. Methane production rates reported were determined only from the initial linear portion of growth curves (R^2 values around 0.83 or greater, with most values above 0.9), eliminating exponential increases of methane production when possible. For all but one site, three or more time points were used to calculate methane production rates. Two time points were used for Cejar 3 due to high methane production rates, where methane concentrations exceeded 1000 ppm and exhibited exponential growth at the time of the third measurement. Determining methane production rates using only two points could lead to misinterpretation of actual production rates, as there is no way to establish if the second time point encompasses any part of the exponential increase.

In order to calculate methane production rates, the ideal gas law was used to convert headspace methane concentrations (ppm) to nanomole (nmol) values. The headspace volume for all serum vials was calculated from the difference between the empty serum vial volume (38 mL) and the calculated volume of slurries (microbial mat or crust plus site water, and inhibitors). To determine the volume of slurries in each vial, the wet densities of microbial mat and crust were determined by the water displacement method, using approximately 3 g to 5 g of sample. Methane production rates are reported in units of $\text{nmol g}^{-1} \text{d}^{-1}$.

3.1.2b. *Stable Carbon Isotopes*

Gas samples were taken from the headspace of the incubation vials and analyzed for $\delta^{13}\text{C}_{\text{CH}_4}$ and $\delta^{13}\text{C}_{\text{CO}_2}$ values on a Hewlett Packard gas chromatograph with a 60 m (for some samples, 30 m) Supel-Q PLOT capillary column in line with a ThermoQuest Finnigan Delta Plus XL isotope-ratio mass spectrometer (IRMS). Incubation vials were thawed and shaken before 25 μL to 13,000 μL was extracted from the incubation vial headspace and injected into the gas chromatograph. For large volume samples (more than 1,000 μL of gas), an equivalent volume of MilliQ water was added simultaneously to the extraction of the gaseous headspace to avoid pulling a vacuum in the vial. The MilliQ water was boiled and cooled to reduce the chance that any dissolved methane and CO_2 would be injected into the sample. The other step necessary to analyze large volumes of gas was the cryofocusing method (Rice et al., 2001). This method lowers IRMS backgrounds and enhances instrument precision for isotopic analysis by concentrating gas samples in an external column before separation of gas occurs in the gas chromatograph. Cryofocusing was used for samples having less than 2000 ppm of the desired gas, in this case, either methane or carbon dioxide.

Analytical precision for methane and carbon dioxide gases were based on repetitive analysis of a 1000 ppm and 3% CH_4 standard, and a 99.99% tank CO_2 standard. Repeated measurements of the 1000 ppm ($n=156$) and 3% CH_4 ($n=132$) standards were $-36.9 \pm 0.3 \text{ ‰}$ and $-36.8 \pm 0.3 \text{ ‰}$, respectively. The nominal value for both the 1000 ppm and 3% CH_4 standards was -36.9 ‰ . Repeat measurements of the CO_2 tank standard ($n=197$) gave an average value of $-23.3 \pm 0.6 \text{ ‰}$. The $\delta^{13}\text{C}_{\text{CO}_2}$ values measured from all

incubation vials were corrected daily based on the isotopic difference of the 99.99% tank CO₂ standard from its nominal value of -22.3 ‰.

3.2. Dissolved Inorganic Carbon

3.2.1. Sample Preparation

Dissolved inorganic carbon content and $\delta^{13}\text{C}_{\text{DIC}}$ values were determined from water samples taken in the field for the Atacama Desert 2013 and Baja 2014 studies. In the field, 2 mL of site water was collected in triplicate for DIC analysis. Collected water samples were passed through a 0.2 μm syringe filter before injection into an evacuated 8 mL serum vial. Water samples were frozen upside down to reduce gas exchange through the septum until time of analysis. Frozen samples may have experienced slight thawing while in transit, but were frozen again once in the laboratory.

After the initial stable carbon isotopes were analyzed from the gaseous headspace of Baja 2014 incubation vials, the DIC content and $\delta^{13}\text{C}_{\text{DIC}}$ values of the water within the vials were also measured. Although water volumes of 2 mL was intended for use in this DIC experiment, water volumes extracted from incubation vials varied due to the difficulty in removing incubation water from the homogenized microbial mat and crust slurry, causing volume measurements to be questionable. Therefore, extracted water volumes were back calculated after the $\delta^{13}\text{C}_{\text{DIC}}$ values were measured. To calculate estimated water volumes, additional water was injected to fill the remaining headspace of the 8 mL DIC serum vials, and then by subtracting the known volume of added acid (see acidification method below) plus the amount of additional water injected, the remaining volume within the vial is occupied by the incubation water sample. Water samples were

refrigerated and stored upside down to reduce gas exchange through the septum until time of analysis.

3.2.2. *Analytical Procedure*

3.2.2a. *Dissolved Inorganic Carbon Concentrations and $\delta^{13}C_{DIC}$ Values*

DIC concentrations and $\delta^{13}C_{DIC}$ values were determined at the University of Missouri on a Hewlett Packard gas chromatograph with a 60 m (or 30 m) capillary column connected to a ThermoQuest Finnigan Delta Plus XL IRMS. Before analysis, DIC samples were thawed and acidified with 2 mL of 30% phosphoric acid to shift all of the inorganic carbon in the water sample to CO₂. The dissolved CO₂ diffused into the headspace as gas until a state of equilibrium was reached. The samples were injected with approximately 5 mL of helium (He) to increase the internal pressure of the vial back to atmospheric, and vortexed for approximately 30 seconds to ensure the sample and acid were fully reacted. Isotopic values were corrected daily based on the difference between the repetitive analysis of a 99.99% tank of CO₂ standard and its nominal value of -22.3 ‰.

DIC concentrations (mM) were calculated using a linear regression curve of integrated 99.99% tank CO₂ standard peak amplitudes from the gas chromatograph. The ideal gas law was used to determine how much carbon (μmol) was in the injected standard (μL). Since the amount of carbon in each injected sample directly correlates with peak size, the amplitude of the sample peak was used to calculate the amount of carbon in each injected sample. The amount of carbon injected (μmol) was divided by the volume of sample injected (μL) and multiplied by the volume of headspace in the serum vial to determine the total mass of carbon in the headspace. The total DIC concentration

was equal to the total mass of carbon (in the headspace) divided by the total volume of water inside the serum vial (2 mL in field sample vials).

DIC production rates were calculated to establish the concentration of all dissolved inorganic carbon species within the incubation vials, and used to establish the amount of inorganic carbon (CO_2 , HCO_3^- , CO_3^{2-}) the microbial mat and crust material was contributing to the CO_2 pool throughout the incubation period. The initial (field site sample = time zero) and final (incubation vial) DIC concentrations were plotted over time and fitted to a linear regression analysis. To get at the total rate of production occurring in each incubation vial, DIC concentrations (mM) were first multiplied by the volume of water in the incubation vial (0.01 L) to determine the total amount of produced DIC. The total amount (mmol) of DIC was divided by the mass of microbial mat or crust material (g). The amount of DIC produced in each sample (mmol/g) was then divided by the incubation time to calculate the DIC production rate. DIC production rates are reported in $\text{nmol g}^{-1} \text{d}^{-1}$.

3.3. Particulate Organic Matter

3.3.1. Sample Preparation

Sub-samples of homogenized microbial mat or crust, used for incubation slurries, were taken in triplicate and analyzed for particulate organic carbon (POC) content and $\delta^{13}\text{C}_{\text{POC}}$ values. Samples were placed in pre-combusted (450°C for 6 hours) 20 mL scintillation vials and refrigerated. At the University of Missouri, samples were dried at approximately 65°C, then homogenized using a mortar and pestle. Following Hedges and Stern (1984), an aliquot of each sample was weighed and acidified adding 2 mL of 10%

HCl on a daily basis for one to two weeks. The time for decarbonation of samples varied depending on the amount of carbonate carbon in each sample. After the removal of all inorganic carbon, detected by the lack of effervescence, the samples were placed back in the oven to dry. Samples were weighed and homogenized again before isotopic analysis was performed.

3.3.2. Analytical Procedure

To obtain concentrations (% POC) and isotopic composition of POC, acetanilide standards and dried samples were weighed into tin capsules and flash combusted on a Carlo Erba NA 1500 Elemental Analyzer attached to a continuous flow interface (Conflo III) and a Thermo Finnigan Delta Plus XL IRMS. Isotopic values were corrected daily based on the difference between the repetitive analyses of the acetanilide standard, $-33.3 \pm 0.08 \text{ ‰}$, and its nominal value of -33.5 ‰ . Acetanilide was also used as an organic carbon standard to estimate POC concentrations (%) in each sample.

3.4. Ion Concentrations

3.4.1. Sample Collection and Preparation

In the field, site water was collected in triplicate and filtered through a $0.2 \text{ }\mu\text{m}$ filter for later ionic concentration analysis. Samples were frozen in 20 mL vials the same day. Frozen samples experienced slight thawing while in transit, and were frozen again upon arrival at the NASA Ames Research Center and the University of Missouri laboratories.

3.4.2. Analytical Procedure

At the University of Missouri, diluted (1:10 to 1:500) water samples were analyzed on a Dionex ICS-3000 ion chromatograph to determine sulfate (SO_4^{2-}) and chloride (Cl^-) concentrations. A 3.5 mM sodium carbonate, 1.0 mM sodium bicarbonate anion eluent was used as the mobile phase. Standards for sulfate and chloride were made using magnesium sulfate heptahydrate and sodium chloride, respectively. Concentrations of standards ranged between 1 mM and 16 mM. Sulfate and chloride concentrations for each sample, reported in millimolar (mM), were calculated based on a linear regression curve from plotted peak areas and concentrations of the sulfate/chloride standards.

3.5. Carbon Mass Balance

3.5.1. The Methane Pool

Although 99 atom% $^{13}\text{CH}_4$ was added to incubation vials, the continual production of methane by methanogens dilutes the CH_4 pool with the lighter isotope (^{12}C), decreasing the overall atom% of the CH_4 pool methanotrophs have to oxidize. This mass balance calculation was done to estimate the final atom% of CH_4 available for oxidation in $^{13}\text{CH}_4$ -amended incubation vials, the assumption is that the methane production rates are the same in both the unamended control and the $^{13}\text{CH}_4$ -amended incubation vials (Equation 5):

$$\begin{aligned} (\text{atom}\% \text{CH}_4\text{-FINAL POOL}) = & [(\text{atom}\% \text{CH}_4\text{-Control}) * (\text{ppm CH}_4\text{-Initial}) + \\ & (\text{atom}\% \text{CH}_4\text{-Labeled}) * (\text{ppm added CH}_4\text{)}_{\text{Labeled}}] / (\text{ppm CH}_4\text{-Final}) \end{aligned} \quad (5)$$

The above terms are defined as: $atom\%CH_{4-FINAL\ POOL}$ is the final atom% of CH₄ in the labeled methane (¹³CH₄) incubations, $atom\%CH_{4-Control}$ is the initial atom% of the methane (CH₄) pool in the control (calculated from the $\delta^{13}C_{CH_4}$ value of the unamended control incubation), $ppm\ CH_{4-Initial}$ is the concentration of methane that would have been in the incubation to start ($ppm\ CH_{4-Final} - ppm\ added\ CH_{4\ Labeled}$), $atom\% CH_{4- Labeled}$ is the amount of labeled methane added to the vials (99 atom%), $ppm\ added\ CH_{4\ Labeled}$ is the initial measurement of methane in the ¹³CH₄-amended incubations, $ppm\ CH_{4-Final}$ is the final concentration of methane (ppm) in the labeled methane (¹³CH₄) incubation, as measured from the last time point.

3.5.2. Carbon Dioxide

The atom% (and $\delta^{13}C_{CO_2}$ value) of the CO₂ produced in ¹³CH₄-amended incubation vials when methane oxidation and DIC production are contributing to the CO₂ pool was calculated. This was done for sites that showed a positive increase in $\delta^{13}C_{CO_2}$ values between unamended controls and the ¹³CH₄ amended incubations. The assumed rate of methane oxidation used in this mass balance equation was based on observed rates found in previous research. The isotopic fractionation between DIC and atmospheric CO₂ ($\delta^{13}C_{DIC}$ value and $\delta^{13}C_{CO_2}$ value), which is approximately -8 ‰ (Fry, 2006), was applied to $\delta^{13}C_{DIC}$ values of the final DIC pool after determining mass balance (Equation 6):

$$\begin{aligned}
 (atom\% DIC_{FINAL\ POOL}) = & [(atom\% DIC_{Field}) * (DIC\ Prod.\ Rate_{Baja}) + \\
 & (atom\% CH_{4-FINAL\ POOL}) * (MO\ rate_{Lit.})] / (DIC\ Prod.\ Rate_{(DIC+Lit.)}) \quad (6)
 \end{aligned}$$

The terms are as follows: $atom\% DIC_{FINAL POOL}$ is the expected atom% of the produced DIC in $^{13}CH_4$ amended incubation vials, $atom\% DIC_{Field}$ is the atom% of the DIC pool in the field site (converted $\delta^{13}C_{DIC}$ values from the field site data), $DIC Prod. Rate_{Baja}$ is the calculated DIC production rate from Area 1 and Area 9 unamended anaerobic controls, $atom\% CH_4_{FINAL POOL}$ is the final atom% of CH_4 in the labeled methane ($^{13}CH_4$) incubations (calculated by Equation 7), $MO rate_{Lit.}$ is the methane oxidation rate chosen from literature, and $DIC Prod. Rate_{(DIC + Lit.)}$ is the combined contribution of DIC into the CO_2 pool through DIC production (^{12}C) and methane oxidation (^{13}C).

3.6. Data Evaluation

Error was estimated on all data: methane production rates, $\delta^{13}C_{CH_4}$ and $\delta^{13}C_{CO_2}$ values, DIC concentrations and $\delta^{13}C_{DIC}$ values, POC concentrations and $\delta^{13}C_{POC}$ values, and anion concentrations. Error is reported as standard deviations of triplicate samples or half of the range between two values, except in the case of DIC incubation concentrations. For DIC concentrations, error was propagated using the equation for simple sums and differences (Equations 7), and for products and quotients (Equation 8) found in Aikens (1978).

$$e_F = \sqrt{(e_x^2 + e_y^2)} \quad (7)$$

$$e_{F/F} = \sqrt{[(e_x/x)^2 + (e_y/y)^2 + (e_z/z)^2]} \quad (8)$$

The terms are defined as follows; in equation 5, e_F is the final propagated error, e_x^2 is the standard deviation or error associated with the first measurement (x) squared, and e_y^2 is the standard deviation or error associated with the second measurement (y) squared. In equation 6, e_F/F is the final propagated error (e_F) divided by the value to which the error belongs (F), e_x/x is the standard deviation or error associated with the first measurement (e_x) divided by the value to which the error belongs (x), e_y/y and e_z/z are the errors associated with the second and third measurements.

Error was propagated for DIC incubation concentrations, because several measurements used for calculating concentration had to be estimated due to the difficulty in extracting sample water. The propagated error was reported if it was larger than the standard deviation of triplicate measurements (or half range of two measurements). Half the range was used when the third data point was lost or unable to be measured due to human error or instrument malfunction.

Statistical analysis of triplicate samples was done to determine significant differences between measured values of unamended controls, inhibitor additions, and $^{13}\text{CH}_4$ experiments. Two statistical calculations were performed in Microsoft Excel. An f-test was used to determine whether the variance between two populations were equal, followed by a two-tailed distribution of a Student's t-test. The Student's t-test was done to obtain P-values, which indicate the probability that two samples are significantly different. A confidence level of 0.05 was used as the threshold for rejecting the null hypothesis, meaning that P-values ≤ 0.05 were statistically different. P-values ≤ 0.05 suggest there is a 95% probability that measured values are not coincidental and considered statistically different. As an example, if a set of two $\delta^{13}\text{C}_{\text{CO}_2}$ values were

compared and generated a P-value > 0.05 , the values could not be considered significantly different. If the P-values were ≤ 0.05 , the $\delta^{13}\text{C}_{\text{CO}_2}$ values could be reported as statistically different from one another.

4 RESULTS

4.1 Field Site Data

4.1.1. Guerrero Negro, Baja California Sur Sites

The Guerrero Negro evaporating ponds showed a variation in water temperatures ranging from 23 °C to 32 °C in 2012, and 22 °C to 23 °C in 2014 (Table 2.1). Salinity measurements in 2012 were 60 ppt, 158 ppt, and 268 ppt, at Areas 1, 9, and 10, respectively. Salinities remained relatively constant for Areas 1 and 9, measuring 64 ppt and 150 ppt in 2014. At Area 9 and 10, the pH measured moderately alkaline at a pH of 8.

4.1.2 Atacama Desert Sites

The field site data for each Atacama site is presented in Table 2.1. The measured water temperatures at each of the Atacama study locations ranged from 3 °C at ET 2 to 31 °C at the bottom water of Llamara pond LL 4. Water temperature varied slightly from surface to bottom waters (near the sediment-water interface) within Llamara pond sites, with lower temperatures near the surface. The largest temperature change from bottom to surface waters was measured in LL 4, a 13 °C difference. Overall, salinities ranged from 10 ppt at the El Tatio geyser field to 132 ppt in the large gypsum crusted pool (site LL 3) at Salar de Llamara.

4.2 Methane Production Rates

4.2.1. Unamended Control Incubations

Methane production rates for unamended anaerobic controls are reported in Table 4.1 and Figure 4.1. The highest methane production rate for Baja 2012 occurred in Area 1, producing $22.5 \text{ nmol g}^{-1} \text{ d}^{-1}$. The lowest rate occurred in Area 1-Deep and 10-Deep samples, resulting in $0.1 \text{ nmol g}^{-1} \text{ d}^{-1}$. Area 10 was the only sample site that did not have a substantial rate of methane production ($0.0 \text{ nmol g}^{-1} \text{ d}^{-1}$), and therefore the results for these samples will not be expanded on in this paper.

The results for sampling material collected from Areas 1 and 9 in Baja 2014 were significantly different from the Baja 2012 samples. In 2014, Area 1 production rates were $86.8 \text{ nmol g}^{-1} \text{ d}^{-1}$, while the methane production rate at Area 9 had decreased to $6.6 \text{ nmol g}^{-1} \text{ d}^{-1}$. Methane production rates for Area 1 and Area 9 aerobic controls, from Baja 2014, had lower rates than anaerobic controls. For Area 1, the aerobic methane production rate was $65.5 \text{ nmol g}^{-1} \text{ d}^{-1}$, and Area 9 was $1.6 \text{ nmol g}^{-1} \text{ d}^{-1}$. The Atacama Desert sites varied from $0.1 \text{ nmol g}^{-1} \text{ d}^{-1}$ (at LL 4) to $296.0 \text{ nmol g}^{-1} \text{ d}^{-1}$ (at ET 2). Methane production rates at Salar de Atacama sites were, on average, greater than Salar de Llamara sites.

4.2.2 $^{13}\text{CH}_4$ -amended Incubations

Methane production rates for anaerobic and aerobic $^{13}\text{CH}_4$ -amended incubations compared to unamended controls are shown in Table 4.1 and Figure 4.1. Anaerobic and aerobic methane production rates produced by $^{13}\text{CH}_4$ incubation vials for Baja (in 2012 and 2014) were all similar to rates produced by their respective (anaerobic or aerobic) unamended control vials.

It is important to note that methane production rates for Atacama Desert 2013 aerobic $^{13}\text{CH}_4$ -amended incubation vials do not have an unamended aerobic control for comparison, as aerobic controls were not prepared for that study. Data from aerobic incubations should not be compared to unamended anaerobic controls. This is due to significant differences between anaerobic and aerobic controls seen in the incubations set up for Baja in 2014. Nevertheless, incubations vials from two Atacama Desert sites showed statistically different methane production rates between anaerobic $^{13}\text{CH}_4$ -amended and unamended control vials. These sites were LL 4 (with an increase of $0.1 \text{ nmol g}^{-1} \text{ d}^{-1}$) and ET 2 (with a decrease of $47 \text{ nmol g}^{-1} \text{ d}^{-1}$). The aerobic $^{13}\text{CH}_4$ -amended vials for LL 4 and ET 2 showed similar changes in methane production rates from their anaerobic $^{13}\text{CH}_4$ -amended counterparts.

4.2.3. *Inhibitor Amendments*

Inhibitors were added to anaerobic and aerobic Baja 2014 sample incubations to determine if changing substrate conditions would enhance methane oxidation. These methane production rates are presented in Table 4.2 and Figure 4.2. Methane production rates varied based on each inhibitor treatment. BES, an inhibitor of methanogenesis, decreased methane production rates from $86.8 \text{ nmol g}^{-1} \text{ d}^{-1}$ in the anaerobic unamended controls of Area 1 to $5.1 \text{ nmol g}^{-1} \text{ d}^{-1}$ in the BES alone treatments, and from $6.6 \text{ nmol g}^{-1} \text{ d}^{-1}$ to $0.0 \text{ nmol g}^{-1} \text{ d}^{-1}$ at Area 9. Aerobic treatments with added BES also showed a decrease in methane production rates from the unamended aerobic controls. For Area 1, methane production rates decreased from $65.5 \text{ nmol g}^{-1} \text{ d}^{-1}$ in aerobic unamended controls to $3.6 \text{ nmol g}^{-1} \text{ d}^{-1}$ when BES was added, while Area 9 production rates went from $1.6 \text{ nmol g}^{-1} \text{ d}^{-1}$ to $0.0 \text{ nmol g}^{-1} \text{ d}^{-1}$. Molybdate, an inhibitor of bacterial SO_4^{2-} reduction, was

used in anaerobic incubations. Methane production rates at Area 1 increased from 86.8 $\text{nmol g}^{-1} \text{d}^{-1}$ in unamended controls to 389.6 $\text{nmol g}^{-1} \text{d}^{-1}$ when molybdate was added, and at Area 9 rates decreased from 6.6 $\text{nmol g}^{-1} \text{d}^{-1}$ in unamended controls to 0.2 $\text{nmol g}^{-1} \text{d}^{-1}$, when molybdate was added. Picolinic acid, an inhibitor of aerobic methane oxidation, was used in aerobic incubations and showed no affect on methane production rates.

While methane production rates from $^{13}\text{CH}_4$ -amended incubations were compared to unamended controls, $^{13}\text{CH}_4$ + inhibitor amendments were compared to corresponding inhibitor controls (incubations with site material and inhibitor). For Area 1, the anaerobic $^{13}\text{CH}_4$ + BES incubations, which was compared to the anaerobic BES alone incubations (5.1 $\text{nmol g}^{-1} \text{d}^{-1}$), was the only statistically different methane production rate, with a decrease in production to 3.4 $\text{nmol g}^{-1} \text{d}^{-1}$. In Area 9, the anaerobic and aerobic $^{13}\text{CH}_4$ + BES incubation treatments were the only statistically different methane production rates, both measuring an increase of 0.1 $\text{nmol g}^{-1} \text{d}^{-1}$ over the BES alone incubations (0.0 $\text{nmol g}^{-1} \text{d}^{-1}$).

Methane production rates for killed control incubation vials are reported in Table 4.3. In all cases, methane production rates were 0.0 $\text{nmol g}^{-1} \text{d}^{-1}$ and/or statistically lower than those occurring in unamended control vials. The killed control incubations that had a rate other than 0.0 $\text{nmol g}^{-1} \text{d}^{-1}$ were: Cejar 1 (-0.1 $\text{nmol g}^{-1} \text{d}^{-1}$), Cejar 2 (0.5 $\text{nmol g}^{-1} \text{d}^{-1}$), CX 1 (-0.2 $\text{nmol g}^{-1} \text{d}^{-1}$), ET 2 (77.1 $\text{nmol g}^{-1} \text{d}^{-1}$), and Baja 2014 Area 1 (0.2 $\text{nmol g}^{-1} \text{d}^{-1}$). Killed control samples that were not statistically different from their unamended control counterpart were LL 3 (0.0 $\text{nmol g}^{-1} \text{d}^{-1}$), LL 8 (0.0 $\text{nmol g}^{-1} \text{d}^{-1}$), and Cejar 1, which was probably due to the relatively high standard deviations of the unamended controls for these locations. The $^{13}\text{CH}_4$ + killed control incubation vials had similar

methane production rates compared to the killed control alone incubations, and are reported in Table 4.3.

4.3 $\delta^{13}\text{C}_{\text{CH}_4}$ Values

4.3.1. Unamended Control $\delta^{13}\text{C}_{\text{CH}_4}$ Values

The $\delta^{13}\text{C}_{\text{CH}_4}$ values for unamended anaerobic controls are reported in Table 4.1 and Figure 4.3. Baja 2012 $\delta^{13}\text{C}_{\text{CH}_4}$ values varied from -61.2 ‰ to -7.4 ‰, from Area 1-Deep and Area 10-Deep, respectively. The other $\delta^{13}\text{C}_{\text{CH}_4}$ values measured -46.7 ‰, from Area 1, and -52.8 ‰ from Area 9. The $\delta^{13}\text{C}_{\text{CH}_4}$ values produced from Baja samples in 2014 were increased in ^{13}C (resulting in higher $\delta^{13}\text{C}_{\text{CH}_4}$ values) compared to the data collected in 2012. Unamended anaerobic controls collected from Area 1 measured -30.1 ‰ and at Area 9 unamended anaerobic controls measured -40.0 ‰. Of the Atacama Desert sites, Salar de Llamara had the largest variation in $\delta^{13}\text{C}_{\text{CH}_4}$ values, from -82.6 ‰ (LL 8) to -20.2 ‰ (LL 2). The $\delta^{13}\text{C}_{\text{CH}_4}$ values for Salara de Atacama sites (Cejar 1, 2, and 3, and CX 1) varied from -30.9 ‰ at CX 1 to -37.8 ‰ at Cejar 2. The $\delta^{13}\text{C}_{\text{CH}_4}$ value at El Tatio was -79.0 ‰.

The $\delta^{13}\text{C}_{\text{CH}_4}$ values for the unamended aerobic controls, set up for Baja sites in 2014, are also reported in Table 4.1 and Figure 4.3. The $\delta^{13}\text{C}_{\text{CH}_4}$ values produced by aerobic controls were similar to those produced by anaerobic controls. At Area 1, the $\delta^{13}\text{C}_{\text{CH}_4}$ value for unamended aerobic controls was -24.4 ‰, and Area 9 was -35.3 ‰.

4.3.2 Inhibitor $\delta^{13}\text{C}_{\text{CH}_4}$ Values

The $\delta^{13}\text{C}_{\text{CH}_4}$ values were measured from inhibitor incubation vials that contained high enough concentrations of methane to be measured (> 50 ppm), and that did not

contain the $^{13}\text{CH}_4$ amendment. This inhibitor data is in Table 4.2, with killed control incubation $\delta^{13}\text{C}_{\text{CH}_4}$ values shown in both Tables 4.2 and 4.3. Only one $\delta^{13}\text{C}_{\text{CH}_4}$ value was measured from the killed control incubations. This was at ET 2, with a $\delta^{13}\text{C}_{\text{CH}_4}$ value of -74.8 ‰.

Of the $\delta^{13}\text{C}_{\text{CH}_4}$ values measured from the Baja 2014 incubations (Table 4.2), one was statistically different from the unamended controls. At Area 1, the $\delta^{13}\text{C}_{\text{CH}_4}$ values in the anaerobic control incubations averaged -30.1 ‰, and in the aerobic control incubations measured -24.4 ‰. The statistically different $\delta^{13}\text{C}_{\text{CH}_4}$ value measured from Area 1 unamended anaerobic control incubations was in the molybdate amendments, which measured -35.3 ‰. The picolinic acid amendment was not statistically different from the unamended aerobic controls and measured -26.6 ‰. For Area 9, the $\delta^{13}\text{C}_{\text{CH}_4}$ values for controls were -39.5 ‰ (anaerobic) and -35.3 ‰ (aerobic). The picolinic acid amendment at Area 9 was the only other $\delta^{13}\text{C}_{\text{CH}_4}$ value measured for Area 9, producing a value of -36.4 ‰, which was not considered statistically different from the unamended aerobic control.

4.4 $\delta^{13}\text{C}_{\text{CO}_2}$ Values

4.4.1 Unamended Control $\delta^{13}\text{C}_{\text{CO}_2}$ Values

The $\delta^{13}\text{C}_{\text{CO}_2}$ values for unamended anaerobic and aerobic controls are presented in Table 4.1 and Figure 4.4. The $\delta^{13}\text{C}_{\text{CO}_2}$ values from all Baja 2012 control incubations were similar, with all values measuring between -14.4 ‰ (at Areas 1 and 9) and -8.9 ‰ (at Area 10-Deep). Anaerobic controls and aerobic controls from Baja 2014 incubation samples also produced similar $\delta^{13}\text{C}_{\text{CO}_2}$ values. At Area 1, the $\delta^{13}\text{C}_{\text{CO}_2}$ values for both

anaerobic and aerobic controls were around -12.3 ‰. At Area 9, $\delta^{13}\text{C}_{\text{CO}_2}$ value for anaerobic controls were -12.9 ‰ and aerobic controls were -15.4 ‰. The decrease in the $\delta^{13}\text{C}_{\text{CO}_2}$ values of the aerobic incubation vials relative to the anaerobic control vials is likely due to increased respiration, brought on by the presence of air (and added oxygen) in the headspace. The $\delta^{13}\text{C}_{\text{CO}_2}$ values produced from controls made of Atacama site materials had more variation; the highest $\delta^{13}\text{C}_{\text{CO}_2}$ value was from ET 2 at +0.1 ‰, and the lowest from LL 4 at -21.7 ‰. Salar de Llamara sites had $\delta^{13}\text{C}_{\text{CO}_2}$ values for unamended control incubations between -21.7 ‰ and -11.7 ‰, averaging about -17 ‰. The control $\delta^{13}\text{C}_{\text{CO}_2}$ values from Salar de Atacama ranged from -16.2 ‰ to -9.3 ‰, averaging slightly higher than Salar de Llamara sites at -13‰.

4.4.2 $^{13}\text{CH}_4$ -amended $\delta^{13}\text{C}_{\text{CO}_2}$ Values

Labeled methane ($^{13}\text{CH}_4$) was added to incubation vials in order to track methane oxidation as positive changes in $\delta^{13}\text{C}_{\text{CO}_2}$ values. The $\delta^{13}\text{C}_{\text{CO}_2}$ values for anaerobic and aerobic $^{13}\text{CH}_4$ amendments are reported in Table 4.1 and Figure 4.4. The maximum difference in $\delta^{13}\text{C}_{\text{CO}_2}$ values between $^{13}\text{CH}_4$ amended incubations and unamended controls were measured in sites LL 2 and LL 4 and Area 9 (2012). The $\delta^{13}\text{C}_{\text{CO}_2}$ value from LL 2 unamended anaerobic control incubations was -11.7 ‰, and the $^{13}\text{CH}_4$ amendments measured -8.0 ‰, which is an increase of +3.7 ‰. The anaerobic control $\delta^{13}\text{C}_{\text{CO}_2}$ value for LL 4 incubations was -21.7 ‰, and the $^{13}\text{CH}_4$ amendments measured -15.0 ‰, which is an increase of +6.7 ‰. The anaerobic control $\delta^{13}\text{C}_{\text{CO}_2}$ value for Area 9 (2012) incubations was -14.4 ‰, and the $^{13}\text{CH}_4$ amendments measured -8.9 ‰, which is an increase of +5.5 ‰. The $\delta^{13}\text{C}_{\text{CO}_2}$ values between the majority of the $^{13}\text{CH}_4$ amended incubations and their unamended controls were about ± 1 ‰. Although several sites are

reported as being statistically different, one aspect of these experiments has to be considered. As noted above, the analytical precision for repeated determinations of the CO₂ standard was ± 0.6 ‰. Therefore, differences in δ¹³C_{CO2} values of ± 1 ‰ become less significant.

4.4.3 *Inhibitor Amended δ¹³C_{CO2} Values*

The δ¹³C_{CO2} values for anaerobic and aerobic inhibitor incubations are presented in Table 4.2 and Figure 4.5. The δ¹³C_{CO2} values for the inhibitor incubations are compared to unamended controls, while ¹³CH₄ + inhibitor incubations are compared to the incubations with the inhibitor alone addition (i.e., ¹³CH₄ + BES vs. BES). Several inhibitor alone incubations have statistically different δ¹³C_{CO2} values, however all δ¹³C_{CO2} values remained within ± 3 ‰ of unamended controls. The largest difference between an unamended control and an inhibitor alone incubation was due to increased methane production when molybdate was added to Area 1 incubations, which had an increase of + 2.8 ‰ from the unamended control. The maximum difference between ¹³CH₄ + inhibitor treated incubations and their corresponding inhibitor alone incubations, was observed between picolinic acid and ¹³CH₄ + picolinic Acid in Area 9. This aerobic experiment had measured -15.1 ‰ (picolinic alone) and -13.4 ‰ (¹³CH₄ + picolinic Acid), which is an increase of + 1.7 ‰.

The δ¹³C_{CO2} values for killed control incubation vials are reported in Table 4.2 and Table 4.3. The δ¹³C_{CO2} values in killed control and ¹³CH₄ + killed-control incubation vials were both statistically lower than those occurring in unamended control vials of Areas 1 and 9. The difference in δ¹³C_{CO2} values between killed controls and unamended

controls was approximately 1 ‰. The $\delta^{13}\text{C}_{\text{CO}_2}$ values measured in $^{13}\text{CH}_4$ + killed-control incubation vials were also similar to those measured in killed control alone incubations.

4.5 Dissolved Inorganic Carbon

4.5.1 Dissolved Inorganic Carbon Concentrations

In this study, DIC data was collected from water sampled in the field and from the water within the incubation vials. The field sample DIC concentrations from Baja 2014 and the Atacama Desert sampling trips are reported in Table 4.4. The DIC concentrations for Areas 1 and 9 are similar at 2.4 mM and 2.0 mM, respectively. DIC concentrations for the Atacama Desert sites ranged from 0.6 mM at LL 8 to 4.2 mM at Cejar 2.

DIC concentrations measured from incubation water samples are reported in Table 4.5. The DIC concentrations from unamended control incubations at Area 1 were about 10 mM higher than the field DIC concentrations, measuring 14.7 mM (anaerobic control) and 15.6 mM (aerobic control). For Area 9, the DIC concentration for the anaerobic controls were 3.5 mM, and was most similar to that measured in the field, while the DIC concentrations in the aerobic incubations measured 7.0 mM. For Area 1, the inhibitor treatments were not significantly different from the corresponding anaerobic and aerobic unamended controls given the high standard deviations/propagated error. However, a few inhibitor treatments from Area 9 were significantly different from their unamended controls. At Area 9, the DIC concentration for the anaerobic inhibitor treatment of molybdate was statistically different, measuring 1.7 mM, which is 1.8 mM lower than the unamended anaerobic controls. The DIC concentrations for the killed

controls were also statistically different from the unamended control at Area 9, measuring 2.2 mM, which is 4.8 mM lower than the unamended aerobic controls.

DIC production rates at Area 1 and Area 9 were calculated using the initial DIC concentrations measured from the field samples and the final DIC concentrations from the incubation water. The calculated DIC production rates for Area 1 incubations were significantly greater than those calculated for Area 9 (Table 4.5). The production rates for Area 1 unamended controls were about $5300 \text{ nmol g}^{-1} \text{ d}^{-1}$, while those at Area 9 were about $100 \text{ nmol g}^{-1} \text{ d}^{-1}$. Statistical differences at Area 1 were observed between the anaerobic $^{13}\text{CH}_4$ + BES amended incubations and the BES alone incubations, with the BES alone treatment measuring $6227 \text{ nmol g}^{-1} \text{ d}^{-1}$ and the $^{13}\text{CH}_4$ + BES treatment measuring $4524 \text{ nmol g}^{-1} \text{ d}^{-1}$. At Area 9, statistically lower DIC production rates were reported for the molybdate incubations compared to corresponding unamended anaerobic controls. DIC production rates for Area 9 molybdate incubations were $-13.1 \text{ nmol g}^{-1} \text{ d}^{-1}$. The killed control incubations at Area 9 measured $6.3 \text{ nmol g}^{-1} \text{ d}^{-1}$, and were also statistically lower than the unamended aerobic control.

4.5.2 $\delta^{13}\text{C}_{\text{DIC}}$ Values

The $\delta^{13}\text{C}_{\text{DIC}}$ values for water samples collected in the field are reported in Table 4.4. At Baja 2014, the field water $\delta^{13}\text{C}_{\text{DIC}}$ value at Area 9 was -1.4 ‰ , and at Area 1 was $+1.9 \text{ ‰}$. Atacama Desert sites had a larger range in $\delta^{13}\text{C}_{\text{DIC}}$ values, from -5.4 ‰ at ET 2 to $+8.7 \text{ ‰}$ at CX 1.

Incubation water samples from unamended control incubations, as well as amended incubation vials, were also analyzed for $\delta^{13}\text{C}_{\text{DIC}}$ values. The anaerobic and aerobic data is reported in Table 4.5. The unamended anaerobic control incubation

$\delta^{13}\text{C}_{\text{DIC}}$ value at Area 1 was -3.0 ‰, and -3.2 ‰ at Area 9. The unamended aerobic control incubation $\delta^{13}\text{C}_{\text{DIC}}$ value was -4.5 ‰ at Area 1, and -4.8 ‰ at Area 9. Incubations with statistically different $\delta^{13}\text{C}_{\text{DIC}}$ values from the unamended controls were the anaerobic BES (-1.4 ‰) and $^{13}\text{CH}_4$ -amended (-1.1 ‰) incubations from Area 9.

4.5.3 Dissolved Inorganic Carbon Production Rates and Mass Balance

DIC production rates were estimated for the sample sites that showed the maximum differences in $\delta^{13}\text{C}_{\text{CO}_2}$ values between unamended anaerobic controls and anaerobic $^{13}\text{CH}_4$ amended incubations. The maximum differences in $\delta^{13}\text{C}_{\text{CO}_2}$ values are +3.7 ‰ at LL 2, +5.5 ‰ at Area 9 (2012), and +6.7 ‰ at LL 4 (Table 4.7). Since the +5.5 ‰ enrichment in $\delta^{13}\text{C}_{\text{CO}_2}$ values at Area 9 (2012) was not replicated in the Baja 2014 incubations, this data was excluded from the mass balance calculations. The DIC production rates for Areas 1 and 9 (Baja 2014) were assumed to be comparable to Salar de Llamara sites that showed enrichments in $\delta^{13}\text{C}_{\text{CO}_2}$ values, because DIC production rate data was not collected for the Atacama Desert 2013 sites.

The atom% of $^{13}\text{CH}_4$ added to the headspace of each incubation vial and the DIC production rates from Baja 2014 incubations were used to determine the mass balance of carbon in the incubation vials (Table 4.7). The estimated atom% of the CH_4 pool in the $^{13}\text{CH}_4$ amended incubation vials ranged from 66 to 90 atom%, which is close to the 99 atom% $^{13}\text{CH}_4$ that was added to the headspace of each vial. The estimated DIC production rates used for LL 2 and LL 4 were based on concentrations of organic matter (% POC) at each site compared to Area 1 and Area 9 (Baja 2014). For example, the estimated DIC production rates for LL 4 were calculated based on Area 1 unamended control incubation rates (about 5300 nmol $\text{g}^{-1} \text{day}^{-1}$), and multiplied accordingly based on

the difference in POC concentrations (Area 1 %POC is 10.1% and LL 4 is 1.7%). The estimated DIC production rate for LL 4 was then $900 \text{ nmol g}^{-1} \text{ day}^{-1}$ for anaerobic samples. The DIC production rates used for LL 2 were based on those observed at Area 9. Since the organic matter compositions at both sites were similar (0.3% at LL 2 and 0.2% at Area 9), the DIC production rates measured at Area 9, $75 \text{ nmol g}^{-1} \text{ day}^{-1}$ for anaerobic samples, were used for site LL 2.

These estimated DIC production rates were used to calculate expected $\delta^{13}\text{C}_{\text{CO}_2}$ values for sites LL 2 and LL 4, assuming an anaerobic methane oxidation rate ($0.05 \text{ nmol g}^{-1} \text{ day}^{-1}$) similar to those observed by Iversen et al. (1987) and Joye et al. (1999) for AOM measured in the water column of Mono and Big Soda Lakes. Using this rate of $0.05 \text{ nmol g}^{-1} \text{ day}^{-1}$, the expected $\delta^{13}\text{C}_{\text{CO}_2}$ values at LL 2 would be approximately +36 ‰, and at LL 4 would be -1 ‰. For the relatively small enrichment observed in $\delta^{13}\text{C}_{\text{CO}_2}$ values between unamended anaerobic controls and anaerobic $^{13}\text{CH}_4$ amended incubation vials, methane oxidation rates for LL 2 and LL 4 are estimated to be $< 0.0001 \text{ nmol g}^{-1} \text{ day}^{-1}$.

4.6 Particulate Organic Matter

4.6.1 Particulate Organic Carbon Concentrations

POC concentrations (%) decreased as salinity increased (Figure 4.6). Sampling sites at higher salinities were made up of evaporite crust (LL 2, LL 3, Cejar 3, Area 9) and contained the lowest levels of POC. Evaporite crust site POC concentrations measured between 0.1 % and 0.3 % (Table 4.4). The lower salinity sites, containing soft microbial mats (LL 4, LL 8, Cejar 1, Cejar 2, CX 1, and Area 1), had higher POC

concentrations. The POC concentrations for these sites ranged between 1.7 % and 12.1 %, with the highest concentrations measured at Area 1.

4.6.2 $\delta^{13}\text{C}_{\text{POC}}$ Values

The range of $\delta^{13}\text{C}_{\text{POC}}$ values at Baja (for both 2012 and 2014 combined) was between -14.7 ‰ and -5.4 ‰, at Area 9 and Area 10-deep, respectively (Table 4.4). Atacama Desert $\delta^{13}\text{C}_{\text{POC}}$ values ranged from -14.5 ‰ at ET 2 to -5.5 ‰ at CX 1.

4.7 Ion Concentrations

Concentrations of chloride (Cl^-) and sulfate (SO_4^{2-}) varied from site to site, and are reported in Table 4.6. Chloride concentrations varied from 127.7 mM to 5400 mM, at ET 2 and Area 10, respectively. Lowest sulfate concentrations were measured from ET 2 at 1.8 mM, and the highest from LL 3 at 231.8 mM. Chloride concentrations increased with increasing salinity, with most samples falling along the line of chloride concentrations expected for evaporating seawater (Figure 4.7). However, Area 10 chloride concentrations fell above the line.

Sulfate concentrations at Atacama sites plotted above the estimated sulfate concentrations expected in evaporating seawater. Sulfate concentrations measured at Baja plot along the line for sulfate concentrations expected from the evaporation of seawater, except for Area 10, which falls short of expected values. Sulfate concentrations measured at Baja also increase with increasing salinity (Figure 4.8).

5 DISCUSSION

The purpose of this study was to determine if microbial methane oxidation occurs in hypersaline environments containing soft microbial mats and evaporite crusts. To address this goal, experiments were set up to test for microbial methane oxidation by tracing $^{13}\text{CH}_4$ into $^{13}\text{CO}_2$. Amendments of $^{13}\text{CH}_4$ and inhibitors were added to anaerobic and aerobic incubation vials containing microbial mat and crust, and the differences in $\delta^{13}\text{C}_{\text{CO}_2}$ values produced in amendment versus control vials were analyzed.

5.1 Site Water Comparisons

A direct linear relationship was observed between chloride concentrations and salinity for Guerrero Negro, Baja California Sur sites (Figure 4.7), suggesting the source water to be of marine origin (seawater). This was determined by plotting the approximate seawater concentrations of chloride (560 mM) and sulfate (29 mM) versus seawater salinity (35 ppt) (Berner and Berner, 2012). However, chloride concentrations at Area 10 plotted above the chloride concentration expected from evaporating seawater. It is unclear as to why Area 10 chloride concentrations fell above the seawater evaporation line. At the Atacama sites, chloride concentrations generally plotted below chloride concentrations expected in evaporating seawater, indicating a non-marine water source (Figure 4.7). The water source for Atacama sites is most likely derived from meteoric precipitation and snowmelt coming from the Andes.

The sulfate concentrations measured at Baja and the Atacama Desert sites (Figure 4.8) also indicate different origins of source water for the localities sampled. Sulfate concentrations at Guerrero Negro (Baja) show increased sulfate concentrations with

increasing salinity, which correlates with the evaporation of marine water (seawater) to the more concentrated crystallization ponds. However, Area 10 has lower sulfate concentrations than expected, which is most likely caused by an increase in the precipitation of gypsum (CaSO_4). Sulfate concentrations for the Atacama sites were scattered, with all site sulfate concentrations above the expected sulfate concentrations for evaporating seawater. Since the snowmelt coming from the Andes is attributed as the main origin of groundwater into the Atacama Desert, the increase in aqueous sulfate concentrations could be linked to high levels of sulfur present in the volcanic Chilean bedrock (Risacher and Fritz, 2009). There were also some minor variations in sulfate concentrations within the ponds (or subset of the pond) at each Atacama salar. In Salar de Llamara, the largest variation was observed in the large gypsum pool, between LL 2 and LL 3, with a difference of 77 mM. The difference in Salar de Atacama sites (Cejar 1 and Cejar 3) was approximately 27 mM. The variation in sulfate concentrations between sampling sites in the same salar could be linked to a difference in sulfate reduction rate by sulfate reducing bacteria.

5.2 Methanogenesis in Hypersaline Ponds

Methane production rates were measured to insure methanogenesis was occurring at each hypersaline study site. The incubations from Area 10 were the exception, with no appreciable methane production observed (Table 4.1, Figure 4.1). Methane production rates in unamended anaerobic controls varied from site to site, producing methane at rates from $0.1 \text{ nmol g}^{-1} \text{ d}^{-1}$ to $296.0 \text{ nmol g}^{-1} \text{ d}^{-1}$. In most cases, methane production rates from anaerobic and aerobic $^{13}\text{CH}_4$ -amended incubation vials were statistically similar to their

unamended control counterparts, with the exception of sites LL 4 and ET 2. At LL 4, methane production rates in anaerobic and aerobic $^{13}\text{CH}_4$ -amended incubation vials increased slightly by about $0.1 \text{ nmol g}^{-1} \text{ d}^{-1}$, while production rates at ET 2 decreased by about $50 \text{ nmol g}^{-1} \text{ d}^{-1}$. It is unclear as to why these sites showed statistically different production rates in the $^{13}\text{CH}_4$ -amended incubation vials.

Incubation experiments were set up to characterize whether anaerobic or aerobic methane oxidation is prevalent in these hypersaline sites. It is suspected that aerobic $^{13}\text{CH}_4$ -amended incubation vials prepared for Atacama Desert 2013 sites, containing relatively high levels of organic matter (POC > 2 %) (LL 8, Cejar 1, Cejar 2, CX 1, ET 2), turned anoxic after incubating for only a few days. This is probably due to high rates of organic matter oxidation that leads to the depletion of O_2 in the incubation system (Eby, 2004). The gypsum crust sites (LL 2, LL 3, Cejar 3) are thought to have remained aerobic due to their relatively low concentrations of organic matter (POC < 2 %) compared to those from organic rich sites. This would explain the variation in methane production rates observed between the anaerobic and aerobic $^{13}\text{CH}_4$ -amended incubation vials of Atacama Desert 2013, in which most 'aerobic' organic rich sites produced more methane than gypsum crusted sites.

For example, aerobic $^{13}\text{CH}_4$ -amended incubation vials prepared with gypsum crust, like LL 2 and 3, appear to have significantly lower methane production rates when compared to their anaerobic counterparts (Figure 4.1). The organic-rich sites, such as CX 1 and ET 1, have similar production rates in anaerobic and aerobic experiments. The aerobic $^{13}\text{CH}_4$ -amended incubation vials containing organic-rich mats (high POC) should not be compared to their unamended anaerobic control counterparts, as they most likely

did not remain aerobic. Instead, data from aerobic incubations should be compared to an unamended aerobic control. Since headspace concentrations of oxygen cannot be accounted for in the Atacama Desert 2013 study, and the aerobic status within the vials is questionable, the aerobic samples will not be discussed further.

The experimental design for preparing aerobic incubations vials was altered for the Baja 2014 study by adding O₂ gas into the headspace of aerobic vials. This was done to ensure aerobic incubation vials remained oxic. Methane production rates measured at Area 1 (organic rich) are similar for all anaerobic and aerobic controls, as well as the ¹³CH₄-amended incubation vials (Figure 4.1). This is curious, as the presence of oxygen in these vials (concentrations > 5 %) should have halted methanogenesis, since methanogens are obligate anaerobes. However, rates occurring in aerobic incubation vials at Area 9 (gypsum crust) are statistically lower from their anaerobic counterparts. These data support the need for aerobic controls, especially when analyzing sites low in organic material (gypsum crust). These data also suggests that systems with increased levels of organic matter have the potential to produce more methane than systems with low organic matter concentrations (Figure 5.1), which has been documented in previous studies (Capone and Kiene, 1988).

The $\delta^{13}\text{C}_{\text{CH}_4}$ values were measured to establish the presence of biogenic methane, and to observe the naturally occurring isotopic composition of methane produced by the local methanogenic communities. Measured $\delta^{13}\text{C}_{\text{CH}_4}$ values were between -20.2 ‰ and -82.6 ‰, with the exception of Area 10-Deep, which measured -7.4 ‰ (Figure 4.3). Most of these values fall below the previously considered biogenic range of methane ~ -110 ‰ to ~ -60 ‰ (Whiticar, 1999). This range has recently been re-evaluated due to studies

showing that biogenic $\delta^{13}\text{C}_{\text{CH}_4}$ values are greater in hypersaline environments, and are caused by decreased fractionation due to substrate limitations (Tazaz, et al., 2013, Kelley et al., 2014).

5.3 $^{13}\text{CH}_4$ -amended Incubations

The $\delta^{13}\text{C}_{\text{CO}_2}$ values do not vary much between unamended control incubations and those with added $^{13}\text{CH}_4$, suggesting that little, if any, of the injected $^{13}\text{CH}_4$ was oxidized into the CO_2 pool (Figure 4.4). The $\delta^{13}\text{C}_{\text{CO}_2}$ values for the majority of $^{13}\text{CH}_4$ -amended incubations were within ~ 1 ‰ of respective controls, which as previously stated is close to the analytical precision for repeated determinations of the CO_2 standard, ± 0.6 ‰. The largest enrichment in $\delta^{13}\text{C}_{\text{CO}_2}$ values occurred at Salar de Llamara sites LL 2 and 4, increasing by about $+3.5$ ‰ and $+6.7$ ‰, respectively. The enrichment in $\delta^{13}\text{C}_{\text{CO}_2}$ values at Area 9 (2012), of $+5.5$ ‰, was not replicated in 2014, and therefore was not investigated further. To investigate the significance of a $+6.7$ ‰, and $+3.5$ ‰ enrichment in the isotopic composition of carbon dioxide, a mass balance of carbon for sites LL 2 and LL 4 was performed (Table 4.7)

5.3.1. Methane

Overall the atom% of CH_4 in $^{13}\text{CH}_4$ amended incubation vials was diluted from the 99 atom% that was added to the incubation vial headspace, to about 60 - 90 atom% (Table 4.7). The methane produced at Salar de Llamara sites LL 2 and LL 4 diluted the $^{13}\text{CH}_4$ pool by no more than 30 atom%, and the majority of available methane in the headspace remained labeled (^{13}C). If methane oxidation were to occur, an observed increase in the isotopic composition of CO_2 should be noticeable.

5.3.2 Methane Oxidation

The DIC production rates calculated in Area 9 (gypsum crusted area) and Area 1 (organic rich) unamended control incubation vials were used to establish a base line rate of produced DIC containing the lighter isotope (^{12}C) for Salar de Llamara sites LL 2 and LL 4. The DIC production rates at Area 1 were substantially greater (50x) compared to the DIC production rates of Area 9, which measured $\sim 100 \text{ nmol g}^{-1} \text{ d}^{-1}$. The greater POC concentrations at Area 1, 10.1 % POC, versus the lesser concentration at Area 9, 0.2 % POC, are thought to have contributed to the observed difference in DIC production rates. Due to the greater levels of organic carbon in the system, respiration of that organic carbon would presumably be greater. Since site LL 2 has a similar crust environment as Area 9, DIC production rates were assumed to be comparable. Site LL 4 was more organic rich than both sites LL 2 and Area 9, but not as organic rich as Area 1, thus a fraction of the DIC production rate from Area 1 was used.

Assuming a methane oxidation rate of $0.05 \text{ nmol g}^{-1} \text{ d}^{-1}$, which is an estimated and relatively conservative rate based on previously published studies of hypersaline lakes by Iversen et al. (1987) and Joye et al. (1999), we can calculate expected $\delta^{13}\text{C}_{\text{CO}_2}$ values if this amount of methane oxidation were to occur in the hypersaline study sites showing the small enrichment of ^{13}C in the CO_2 pool (LL 2, LL 4). The expected $\delta^{13}\text{C}_{\text{CO}_2}$ values for anaerobic $^{13}\text{CH}_4$ amended incubation vials would be about +36 ‰ at LL 2, and -1 ‰ at LL 4 (Table 4.7). This means that the enrichment in $\delta^{13}\text{C}_{\text{CO}_2}$ values between the $^{13}\text{CH}_4$ amended incubation vials and unamended controls should have been in the range of +50 and +20 ‰, at sites LL 2 and LL 4, respectively, not the measured +3.5 ‰ to +6.7 ‰.

Compared to these expected $\delta^{13}\text{C}_{\text{CO}_2}$ values, the small ^{13}C enrichment measured in the CO_2 pool at our hypersaline study sites (max +6.7 ‰) suggests that if methane oxidation were occurring it would be lower than $0.05 \text{ nmol g}^{-1} \text{ day}^{-1}$ (estimated rate based on measurements made by Iversen et al. (1987) and Joye et al. (1999)). Given the small enrichment in $\delta^{13}\text{C}_{\text{CO}_2}$ values, the estimated methane oxidation rates at sites LL 2 and LL 4 is $< 0.0001 \text{ nmol g}^{-1} \text{ d}^{-1}$. The estimated methane oxidation rates at sites LL 2 and LL 4 were determined by using the mass balance of carbon equation (Equation 6). Instead of using the literature based methane oxidation rate, based on Iversen et al. (1987) and Joye et al. (1999), estimated rates (such as $0.0001 \text{ nmol g}^{-1} \text{ d}^{-1}$) were plugged into the Equation 6 until $\delta^{13}\text{C}_{\text{CO}_2}$ values for $^{13}\text{CH}_4$ amended incubation vials were close to equalling the measured values.

Since DIC production rates occurring within the incubation vials was exceptionally greater than the rate of methane oxidation, the $\delta^{13}\text{C}_{\text{CO}_2}$ values were flooded with ^{12}C , diluting any enrichment in ^{13}C to the CO_2 pool of samples with added $^{13}\text{CH}_4$. However, the low DIC production rates in the gypsum crusted sites allowed for a small enrichment in $\delta^{13}\text{C}_{\text{CO}_2}$ values to be observed, while organic rich sites with high DIC production rates, like Area 1, showed no enrichment in $\delta^{13}\text{C}_{\text{CO}_2}$ values. It is possible that small enrichments of ^{13}C occurred in the CO_2 pool at the organic rich sites, but that high DIC production rates (of ^{12}C) overwhelmed any ^{13}C enrichment. This would cause changes in $\delta^{13}\text{C}_{\text{CO}_2}$ values to become less apparent.

5.4 Inhibitor and $^{13}\text{CH}_4$ + Inhibitor Amendments

To further investigate the +5.5 ‰ enrichment in $\delta^{13}\text{C}_{\text{CO}_2}$ values at Area 9 (2012), inhibitors were introduced to Guerrero Negro, Baja California Sur incubation vials in 2014 (Table 3.1). Inhibitor treatments were added to determine if methanotrophs would be more or less active under different substrate conditions, and to observe these effects with the addition of $^{13}\text{CH}_4$. Observations were also made under oxic and anoxic conditions, to determine if anaerobic or aerobic methane oxidation is the dominant oxidation pathway occurring in these hypersaline sites. The effectiveness of each inhibitor was evaluated based on changes in methane production rates and $\delta^{13}\text{C}_{\text{CO}_2}$ values (Figure 4.2 and 4.5).

Sodium molybdate was added to incubation vials to stop anaerobic microbial sulfate reduction, which studies suggest is coupled with anaerobic methane oxidation (Orphan et al., 2001, Knittel and Boetius, 2009). Adding molybdate statistically increased the rate of methanogenesis in Area 1 incubations, but had no effect on methanogenesis at Area 9 (Figure 4.2). The two possible effects molybdate could have had on methane oxidation are (1) due to the inhibition of sulfate reduction, methane oxidation would also be inhibited, and (2) methane oxidation is not exclusively dependent on sulfate-reducing bacteria and are using other known electron acceptors (such as NO_3^-), and that by giving methanogens a chance to become more active, methane oxidation would increase with increasing levels of dissolved methane. As a result of the inhibition of sulfate reducers, methanogenesis activity would increase: (1) if methane oxidation was also inhibited, we would see no change in methane production rates or $\delta^{13}\text{C}_{\text{CO}_2}$ values between the molybdate and $^{13}\text{CH}_4$ + molybdate incubations; (2) if methane oxidation was not

dependent on sulfate reduction, and methane oxidation were occurring, we would see a decline in methane production rates in molybdate treatments versus unamended controls. Also observed would have been an enrichment in $\delta^{13}\text{C}_{\text{CO}_2}$ values between the $^{13}\text{CH}_4$ + molybdate incubations compared to molybdate-alone incubations. An enrichment in $\delta^{13}\text{C}_{\text{CO}_2}$ values of the $^{13}\text{CH}_4$ + molybdate incubations would show the ^{13}C of the added $^{13}\text{CH}_4$ was being incorporated into the CO_2 pool. Due to these different effects, the changes in methane production rates and lack of change observed in $\delta^{13}\text{C}_{\text{CO}_2}$ values for molybdate treatments, these experiments are difficult to interpret in relation to methane oxidation. Additional data, such as the identification of any methanotrophs (either anaerobic or aerobic) would help conclude to what extent methane oxidation is occurring at these sites.

Bromoethanesulfonate (BES), a specific inhibitor of methanogens, was used to inhibit methanogenesis and to observe the effects methane oxidation could have on $\delta^{13}\text{C}_{\text{CO}_2}$ values (Figure 4.5). Stopping methane production and adding $^{13}\text{CH}_4$ to incubation vials, increases the chances that if any methane oxidation were occurring in these hypersaline environments, the ^{13}C of the added methane would be detectable in the CO_2 pool. The addition of BES effectively inhibited methanogenesis at both Areas 1 and 9, however the $\delta^{13}\text{C}_{\text{CO}_2}$ values for $^{13}\text{CH}_4$ + BES treatments failed to show signs of methane oxidation. This suggest that very little, if any methane oxidation is occurring in these hypersaline sites.

Picolinic acid is an inhibitor of aerobic methane oxidation and was used to determine the role aerobic methane oxidation plays in these hypersaline environments. Aerobic methane oxidation does not appear to effect methane production rates or $\delta^{13}\text{C}_{\text{CO}_2}$

values from unamended controls, suggesting no aerobic oxidation of methane occurred at either Areas 1 or 9 (Figure 4.5). This was somewhat expected based on previous research, which shows the majority of methane oxidation occurring in hypersaline environments, occurs under anoxic conditions (Joye, et al., 1999, Iverson, et al., 2007, Maignien, et al., 2013).

Overall, the $^{13}\text{CH}_4$ + inhibitor incubations showed no deviation from controls (inhibitor-alone incubations) for methane production rates or $\delta^{13}\text{C}_{\text{CO}_2}$ values, supporting two possible conclusions. First, methanotrophs are present, but methane oxidation is not occurring at high enough rates to affect stable carbon isotope values and methane production rates. The alternative possibility is that methanotrophs simply do not occur at these hypersaline sites.

6. CONCLUSION

The isotopic composition of carbon dioxide produced by microbes in organic rich and gypsum crusted hypersaline ponds located near Guerrero Negro, Baja California Sur, Mexico, and the Atacama Desert in northern Chile, were analyzed for evidence of anaerobic and aerobic methane oxidation. Carbon dioxide production rates and $\delta^{13}\text{C}_{\text{CO}_2}$ values were measured from incubation vials with added 99 atom% $^{13}\text{CH}_4$, site sediment, mat, or crust, and water. Sites containing relatively low levels of particulate organic carbon showed a slight enrichment of ^{13}C in the CO_2 pool when $^{13}\text{CH}_4$ was added. This enrichment, of approximately +4 ‰ and +7 ‰, was not high enough to be considered a result of methane oxidation, as estimated $\delta^{13}\text{C}_{\text{CO}_2}$ values should have increased by at least +20 ‰ to +50 ‰ if methane oxidation were occurring at similar levels as seen in other hypersaline sites (based on measurements by Iversen et al. (1987) and Joye et al. (1999), $0.05 \text{ nmol g}^{-1} \text{ day}^{-1}$). This small enrichment in $\delta^{13}\text{C}_{\text{CO}_2}$ values is credited in part by the relatively high production rates of dissolved inorganic carbon, which flooded the CO_2 pool and $\delta^{13}\text{C}_{\text{CO}_2}$ values with the lighter isotope (^{12}C). If methane oxidation were occurring at these hypersaline sites, it would be $< 0.0001 \text{ nmol g}^{-1} \text{ d}^{-1}$.

Although little to no evidence for methane oxidation was observed in these hypersaline ponds, this research expands on the few studies that have investigated methane oxidation in hypersaline environments (Iverson, et al., 1987, Joye, et al., 1999, Maignien, et al., 2013). It also lends itself to understanding the potential influence methane oxidation could have on isotopic compositions produced by microbial communities in hypersaline areas.

7. REFERENCES

- Aikens, D.A. (1978). *Integrated Experimental Chemistry: Principles and techniques*. Allyn & Bacon, Incorporated. 42-63.
- Bebout, B.M., Hoehler, T.M., Thamdrup, B., Albert, D., Carpenter, S.P., Hogan, M., Hogan, M., Turk K., & Des Marais, D.J. (2004). Methane production by microbial mats under low sulphate concentrations. *Geobiology*, 2(2):87-96.
- Bedard C. and Knowles R. (1989). Physiology, biochemistry, and specific inhibitors of CH₄, NH₄⁺, and CO oxidation by methanotrophs and nitrifiers. *Microbiological Reviews* 53:68–84.
- Berner, E. K., & Berner, R. A. (2012). *Global environment: water, air, and geochemical cycles*. Princeton University Press.
- Bodelier, P.L., & Frenzel, P. (1999). Contribution of methanotrophic and nitrifying bacteria to CH₄ and NH₄⁺ oxidation in the rhizosphere of rice plants as determined by new methods of discrimination. *Applied and Environmental Microbiology*, 65(5): 1826-1833.
- Boetius, A., Ravensschlag, K., Schubert, C.J., Rickert, D., Widdel, F., Gieseke, A., Amann, R., Jørgensen, B.B., Witte, U., & Pfannkuche, O. (2000). A marine microbial consortium apparently mediating anaerobic oxidation of methane. *Nature*, 407(6804):623-626.
- Capone, D.G., & Kiene, R.P. (1988). Comparison of microbial dynamics in marine and freshwater sediments: Contrasts in anaerobic carbon catabolism. *Limnology and Oceanography*, 33(4):725-749.
- Chowdhury, T. R., & Dick, R. P. (2013). Ecology of aerobic methanotrophs in controlling methane fluxes from wetlands. *Applied Soil Ecology*, 65:8-22.
- Cicerone, R.J., & Oremland, R.S. (1988). Biogeochemical aspects of atmospheric methane. *Global Biogeochemical Cycles*, 2(4):299-327.
- Demergasso, C., Casamayor, E. O., Chong, G., Galleguillos, P., Escudero, L., & Pedrós-Alió, C. (2004). Distribution of prokaryotic genetic diversity in athalassohaline lakes of the Atacama Desert, Northern Chile. *FEMS Microbiology Ecology*, 48(1):57-69.
- Demergasso, C., C. Dorador, D. Meneses, J. Blamey, N. Cabrol, L. Escudero, and G. Chong. (2010). Prokaryotic diversity pattern in high-altitude ecosystems of the Chilean Altiplano, *Journal of Geophysical Research*, 115, G00D09: doi:10.1029/2008JG000836.

- Dunckel, A.E., Cardenas, M.B., Sawyer, A.H., & Bennett, P.C. (2009). High-resolution in-situ thermal imaging of microbial mats at El Tatio Geysir, Chile shows coupling between community color and temperature. *Geophysical Research Letters*, 36(23).
- Fernandez-Turiel, J.L., Garcia-Valles, M., Gimeno-Torrente, D., Saavedra-Alonso, J., & Martinez-Manent, S. (2005). The hot spring and geyser sinters of El Tatio, Northern Chile. *Sedimentary Geology*, 180(3):125-147.
- Fry, Brian. (2006). Stable isotope ecology. New York: Springer: Vol. 521. Chapter 3.
- Hanson, R.S., & Hanson, T.E. (1996). Methanotrophic bacteria. *Microbiological Reviews*, 60(2):439-471.
- Hedges J.I. and Stern J.H. (1984). Carbon and nitrogen determinations of carbonate-containing solids. *Limnology and Oceanography*. 29:657–663.
- Heyer, J., Berger, U., Hardt, M., & Dunfield, P.F. (2005). *Methylohalobius crimeensis* gen. nov., sp. nov., a moderately halophilic, methanotrophic bacterium isolated from hypersaline lakes of Crimea. *International Journal of Systematic and Evolutionary Microbiology*, 55(5):1817-1826.
- Hoehler, T.M., Alperin, M.J., Albert, D.B., & Martens, C.S. (1994). Field and laboratory studies of methane oxidation in an anoxic marine sediment: Evidence for a methanogen-sulfate reducer consortium. *Global Biogeochemical Cycles*, 8(4):451-463.
- Iversen, N., & Jorgensen, B.B. (1985). Anaerobic methane oxidation rates at the sulfate-methane transition in marine sediments from Kattegat and Skagerrak (Denmark). *Limnology and Oceanography*, 30(5):944-955.
- Iversen, N., Oremland, R.S., & Klug, M.J. (1987). Big Soda Lake (Nevada). 3. Pelagic methanogenesis and anaerobic methane oxidation. *Limnology and Oceanography*, 32(4):804-8.
- Jones, B., & Renaut, R.W. (1997). Formation of silica oncoids around geysers and hot springs at El Tatio, northern Chile. *Sedimentology*, 44(2):287-304.
- Joye, S.B., Connell, T.L., Miller, L.G., Oremland, R.S., & Jellison, R.S. (1999). Oxidation of ammonia and methane in an alkaline, saline lake. *Limnology and Oceanography*, 44(1):178-188.
- Kelley, C.A., Poole, J.A., Tazaz, A.M., Chanton, J.P., and Bebout, B.M. (2012). Substrate Limitation for Methanogenesis in Hypersaline Environments. *Astrobiology*, 12(2):89-97.
- Kelley, C.A., Nicholson, B.E., Beaudoin, C.S., Detweiler, A.M., & Bebout, B.M. (2014). Trimethylamine and organic matter additions reverse substrate limitation effects on

- the $\delta^{13}\text{C}$ values of methane produced in hypersaline microbial mats. *Applied and Environmental Microbiology*, AEM-02641.
- Killops, S.D., & Killops, V.J. (2005). *Introduction to Organic Geochemistry*, Second Edition. Blackwell Publishing: 94, 144-162.
- King, G. M. (1984). Metabolism of trimethylamine, choline, and glycine betaine by sulfate-reducing and methanogenic bacteria in marine sediments. *Applied and Environmental Microbiology*, 48(4):719-725.
- Knittel, K., & Boetius, A. (2009). Anaerobic oxidation of methane: progress with an unknown process. *Annual review of microbiology*, 63:311-334.
- Lidstrom, M.E., & Somers, L. (1984). Seasonal study of methane oxidation in Lake Washington. *Applied and Environmental Microbiology*, 47(6):1255-1260.
- Maignien, L., Parkes, R.J., Cragg, B., Niemann, H., Knittel, K., Coulon, S., Akhmetzhanov, A., & Boon, N. (2013). Anaerobic oxidation of methane in hypersaline cold seep sediments. *FEMS Microbiology Ecology*, 83(1):214-231.
- McKay, C.P., Friedmann, E.I., Gomez-Silva, B., Caceres-Villanueva L., Andersen D., and Landheim, R. (2003), Temperature and moisture conditions for life in the extreme arid region of the Atacama Desert: Four years of observations including the El Niño of 1997–1998, *Astrobiology*, 3:393 – 406.
- Oremland, R.S., Marsh, L., & DesMarais, D.J. (1982). Methanogenesis in Big Soda Lake, Nevada: an alkaline, moderately hypersaline desert lake. *Applied and Environmental Microbiology*, 43(2):462-468.
- Oremland, R.S. and Capone, D.G. (1988). Use of “specific” inhibitors in biogeochemistry and microbial ecology. *Advances in Microbial Ecology*, 10:285-383.
- Oren, A. (1999). Bioenergetic aspects of halophilism. *Microbiology and Molecular Biology Reviews*, 63(2):334-348.
- Oren, A. (2001). The bioenergetic basis for the decrease in metabolic diversity at increasing salt concentrations: implications for the functioning of salt lake ecosystems. *Hydrobiologia*, 466(1-3):61-72.
- Oren, A. (2011). Thermodynamic limits to microbial life at high salt concentrations. *Environmental Microbiology*, 13(8):1908-1923.
- Orphan, V. J., House, C. H., Hinrichs, K. U., McKeegan, K. D., & DeLong, E. F. (2001). Methane-consuming archaea revealed by directly coupled isotopic and phylogenetic analysis. *Science*, 293(5529):484-487.

- Pueyo, J.J., Chong, G., & Jensen, A. (2001). Neogene evaporites in desert volcanic environments: Atacama Desert, northern Chile. *Sedimentology*, 48(6):1411-1431.
- Reeburgh, W.S. (2007). Oceanic methane biogeochemistry. *Chemical Reviews*, 107:486-513.
- Rice, A.L., Gotoh, A.A., Ajie, H.O., & Tyler, S.C. (2001). High-precision continuous-flow measurement of $\delta^{13}\text{C}$ and δD of atmospheric CH_4 . *Analytical Chemistry*, 73(17):4104-4110.
- Risacher, F., & Fritz, B. (2009). Origin of salts and brine evolution of Bolivian and Chilean salars. *Aquatic Geochemistry*, 15(1-2):123-157.
- Rothschild, L.J., Giver, L.J., White, M.R., & Mancinelli, R.L. (1994). Metabolic activity of microorganisms in evaporites. *Journal of Phycology*, 30(3):431-438.
- Shumilin, E., Grajeda-Muñoz, M., Silverberg, N., Sapozhnikov, D., (2002). Observations on trace element hypersaline geochemistry in surficial deposits of evaporation ponds of Exportadora de Sal, Guerrero Negro, Baja California Sur, Mexico. *Marine Chemistry*, 79:133-153.
- Smith, M.L., Claire, M.W., Catling, D.C., & Zahnle, K.J. (2014). The formation of sulfate, nitrate and perchlorate salts in the martian atmosphere. *Icarus*, 231:51-64.
- Spear, J.R., Ley, R.E., Berger, A.B., & Pace, N.R. (2003). Complexity in natural microbial ecosystems: the Guerrero Negro experience. *The Biological Bulletin*, 204(2):168-173.
- Tazaz, A.M., Bebout, B.M., Kelley, C.A., Poole, J., & Chanton, J.P. (2013). Redefining the isotopic boundaries of biogenic methane: Methane from endoevaporites. *Icarus*, 224(2):268-275.
- Ward, B.B., & Kilpatrick, K.A. (1993). Methane oxidation associated with mid-depth methane maxima in the Southern California Bight. *Continental Shelf Research*, 13(10):1111-1122.
- Whiticar, M.J., Faber, E., & Schoell, M. (1986). Biogenic methane formation in marine and freshwater environments: CO_2 reduction vs acetate fermentation—Isotope evidence. *Geochimica et Cosmochimica Acta*, 50(5):693-709.
- Whiticar, Michael J. (1999), Carbon and hydrogen isotope systematics of bacterial formation and oxidation of methane, *Chemical Geology*, 161:291-314

8. TABLES

Table 2.1: Sampling date, water temperatures (°C), salinity (ppt), pH, and site descriptions for pond sites in Guerrero Negro, Baja California Sur, Mexico, and the Atacama Desert, Chile. Temperatures measured in surface waters are in **bold**, otherwise temperatures were taken near the sediment-water interface.

Sample Site	Date Sampled	Water Temperature (°C)	Salinity (ppt)	pH	Site Description	
Atacama Desert	LL2	May 2013	19 , 22	128	n.d. ¹	Hard gypsum crust, from middle of large shallow pool.
	LL3	May 2013	21 , 23	132	n.d.	Large gypsum crust from opposing end of same pool as LL 2.
	LL4	May 2013	18 , 31	124	n.d.	Small sulfidic pool. Soft crust contained with lots of
	LL8	May 2013	18 , 26	55	n.d.	Soft crust contained purple in the sediment.
	Cejar 1	May 2013	20	45	n.d.	Shallow area. Soft mat with a white and pinkish crust.
	Cejar 2	May 2013	22	54	n.d.	Shallow channel like area. Soft mat with wavy layers.
	Cejar 3	May 2013	13	77	n.d.	Shallow edge of the deep center pool. Gypsum heads with layers of green and red microbial communities.
	CX1	May 2013	20	102	n.d.	Shallow, soft organic rich mat with a tinge of pink.
ET2	May 2013	3	10	n.d.	Small pool containing organic rich sediment.	
Guerrero Negro, Baja California	1	October 2012 March 2014	28 22	60 64	n.d.	Thin organic rich microbial mat (about 2-3 cm thick).
	9	November 2012 March 2014	23 23	158 150	7.6 8.1	Gypsum heads with layers of green and red microbial communities.
	10	November 2012	27 , 32	268	7.9	Gypsum heads on top of flat gypsum/halite crust

¹n.d. = not determined

Table 3.1: Incubation vials prepared in triplicate are denoted by an “X” for sampling locations in Guerrero Negro, Baja California Sur, Mexico, and the Atacama Desert, Chile. Baja 2014 samples denoted with an (*) indicate $^{13}\text{CH}_4$ was also added to inhibitor incubations vials in triplicate to create $^{13}\text{CH}_4$ +inhibitor treatments.

Study Sites	Unamended Controls				Killed Controls	$^{13}\text{CH}_4$ Treatments				Inhibitors						
	Anaerobic		Aerobic			Anaerobic		Aerobic		BES		Molybdate		Picolinic Acid		
	Anaerobic	Aerobic	Anaerobic	Aerobic		Anaerobic	Aerobic	Anaerobic	Aerobic	Anaerobic	Aerobic	Anaerobic	Aerobic	Anaerobic	Aerobic	
Atacama Desert (2013)	LL2	X			X	X										
	LL3	X			X	X										
	LL4	X			X	X										
	LL8	X			X	X										
	Cejjar 1	X			X	X										
	Cejjar 2	X			X	X										
	Cejjar 3	X			X	X										
	CX1	X			X	X										
ET2	X			X	X											
Baja (2012)	1	X				X										
	1-Deep	X				X										
	9	X			X	X										
	10	X			X	X										
Baja (2014)	10-Deep	X			X	X										
	1	X			X*	X*									X*	
Baja (2014)	9	X			X*	X*										X*

Table 4.1: Methane production rates, $\delta^{13}C_{CH_4}$ values, and $\delta^{13}C_{CO_2}$ values for unamended anaerobic and aerobic incubations, as well as $^{13}CH_4$ -amended incubation vials. Error estimates, in parenthesis, are reported as standard deviations of triplicate samples or half of the range of duplicate samples. The bolded values are statistically different, p values < 0.05 , from unamended controls. The aerobic $^{13}CH_4$ -amended Atacama Desert 2013 samples were compared to anaerobic controls.

Sample Site	Material Incubated	Controls				$^{13}CH_4$ Treatments						
		Methane Production Rates (mmol g ⁻¹ d ⁻¹)		$\delta^{13}C_{CH_4}$ Values (‰)		Methane Production Rates (mmol g ⁻¹ d ⁻¹)		$\delta^{13}C_{CO_2}$ Values (‰)				
		Anaerobic	Aerobic	Anaerobic	Aerobic	Anaerobic	Aerobic	Anaerobic	Aerobic			
Atacama Desert (2013)	LL2	crust	1.1 (0.4)	n.d. ¹	-20.2 (2.7)	n.d.	-11.7 (0.3)	n.d.	1.0 (0.2)	0.2 (0.0)	-8.0 (1.4)	-9.3 (0.5)
	LL3	crust	4.0 (2.5)	n.d.	-43.9 (13.1)	n.d.	-13.5 (2.0)	n.d.	2.8 (1.0)	0.2 (0.1)	-10.3 (0.6)	-13.3 (0.7)
	LL4	soft mat	0.1 (0.0)	n.d.	-45.7 (0.2)	n.d.	-21.7 (0.3)	n.d.	0.2 (0.0)	0.3 (0.0)	-15.0 (0.1)	-15.9 (0.7)
	LL8	soft mat	1.3 (0.7)	n.d.	-82.6 (0.3)	n.d.	-20.3 (3.7)	n.d.	1.1 (0.5)	1.6 (0.1)	-21.2 (2.9)	-20.7 (6.3)
	Cejar 1	soft mat	22.5 (18.5)	n.d.	-33.1 (5.0)	n.d.	-16.2 (0.3)	n.d.	4.3 (6.1)	6.7 (1.0)	-15.3 (0.2)	-15.4 (0.3)
	Cejar 2	soft mat	7.7 (0.9)	n.d.	-37.8 (1.0)	n.d.	-14.9 (0.4)	n.d.	19.9 (9.6)	18.5 (8.1)	-13.8 (0.3)	-17.0 (4.2)
	Cejar 3	crust	1.0 (0.1)	n.d.	-34.8 (4.2)	n.d.	-11.1 (0.3)	n.d.	1.0 (0.2)	1.1 (0.3)	-10.6 (0.7)	-12.7 (0.1)
	CX1	soft mat	30.2 (4.5)	n.d.	-30.9 (0.8)	n.d.	-9.3 (1.0)	n.d.	26.1 (12.7)	19.3 (4.6)	-9.7 (0.1)	-9.8 (0.2)
	ET2	sediment	296.0 (4.7)	n.d.	-79.0 (0.3)	n.d.	0.1 (0.1)	n.d.	249.0 (7.2)	214.2 (8.7)	0.7 (0.5)	-4.9 (0.6)
	1	soft mat	22.5 (3.8)	n.d.	-46.7 (1.3)	n.d.	-14.4 (0.2)	n.d.	15.6 (2.7)	n.d.	-14.9 (0.7)	n.d.
Baja (2012)	1-Deep	sediment	0.1 (0.0)	n.d.	-61.2 (1.6)	n.d.	-13.7 (0.5)	n.d.	0.6 (0.3)	n.d.	-15.1 (1.2)	n.d.
	9	crust	21.5 (5.5)	n.d.	-52.8 (4.7)	n.d.	-14.4 (0.4)	n.d.	17.4 (3.1)	n.d.	-8.9 (0.3)	n.d.
	10	crust	0.0 (0.0)	n.d.	-74.9 (0.7)	n.d.	-14.7 (1.9)	n.d.	0.0 (0.0)	n.d.	-14.6 (1.2)	n.d.
Baja (2014)	10-Deep	sediment	0.1 (0.0)	n.d.	-7.4 (1.6)	n.d.	-8.9 (1.5)	n.d.	0.1 (0.0)	n.d.	-9.1 (0.9)	n.d.
	1	soft mat	86.8 (31.8)	65.5 (8.9)	-30.1 (1.0)	-24.4 (2.2)	-12.3 (0.6)	-12.4 (0.1)	90.0 (21.1)	71.5 (16.4)	-12.9 (0.2)	-12.4 (0.2)
9	crust	6.6 (3.8)	1.6 (0.4)	-40.0 (13.6)	-35.3 (4.0)	-12.9 (0.6)	-15.4 (0.5)	10.2 (1.2)	1.40 (0.6)	-11.8 (0.8)	-14.0 (0.4)	

¹n.d. = not determined

Table 4.2: Methane production rates, $\delta^{13}\text{C}_{\text{CH}_4}$ values, and $\delta^{13}\text{C}_{\text{CO}_2}$ values for all Guerrero Negro, Baja 2014 incubations. Error estimates are in parenthesis and reported as standard deviations of triplicate samples or half of the range of duplicate samples. The bolded and italicized values are statistically different, p values < 0.05 , from unamended controls, while the bolded $^{13}\text{CH}_4$ +Inhibitor values are statistically different from their corresponding inhibitor alone treatment (i.e., $^{13}\text{CH}_4$ +BES vs. BES).

Guerrero Negro, Baja (2014)							
Incubation Samples	Methane Production Rates (nmol g ⁻¹ d ⁻¹)		$\delta^{13}\text{C}_{\text{CH}_4}$ Values (‰)		$\delta^{13}\text{C}_{\text{CO}_2}$ Values (‰)		
	Area 1	Area 9	Area 1	Area 9	Area 1	Area 9	
Controls							
Anaerobic Control	86.8 (31.8)	6.6 (3.8)	-30.1 (1.0)	-39.5 (13.6)	-12.3 (0.6)	-12.9 (0.6)	
Aerobic Control	65.5 (8.9)	1.6 (0.4)	-24.4 (2.2)	-35.3 (4.0)	-12.4 (0.1)	-15.4 (0.5)	
Amended Treatments							
Anaerobic	BES	5.1 (0.8)	0.0 (0.0)	n.d. ¹	n.d.	-11.7 (0.3)	-11.6 (0.2)
	Molybdate	389.6 (68.4)	0.2 (0.2)	-35.2 (1.0)	n.d.	-9.5 (0.2)	-14.3 (1.9)
	$^{13}\text{CH}_4$	90.0 (21.1)	10.2 (1.2)	n.d.	n.d.	-12.9 (0.2)	-11.8 (0.8)
	$^{13}\text{CH}_4$ + BES	3.4 (0.7)	0.1 (0.0)	n.d.	n.d.	-12.2 (0.3)	-12.9 (0.4)
	$^{13}\text{CH}_4$ + Molybdate	353.6 (29.1)	0.3 (0.1)	n.d.	n.d.	-9.0 (0.4)	-12.3 (0.9)
	BES	3.6 (0.7)	0.0 (0.0)	n.d.	n.d.	-11.6 (0.3)	-15.6 (0.2)
Aerobic	Picolinic Acid	87.8 (23.3)	1.7 (0.1)	-26.6 (0.7)	-36.4 (0.5)	-12.9 (0.3)	-15.1 (0.4)
	Killed Control	0.2 (0.1)	0.0 (0.0)	n.d.	n.d.	-11.2 (0.6)	-11.7 (0.8)
	$^{13}\text{CH}_4$	71.5 (16.4)	1.4 (0.6)	n.d.	n.d.	-12.4 (0.2)	-14.0 (0.4)
	$^{13}\text{CH}_4$ + BES	3.3 (10.4)	0.1 (0.0)	n.d.	n.d.	-12.0 (0.4)	-13.9 (0.3)
	$^{13}\text{CH}_4$ + Picolinic Acid	76.2 (16.5)	1.4 (0.3)	n.d.	n.d.	-12.0 (0.2)	-13.4 (0.1)
	$^{13}\text{CH}_4$ + Killed Control	0.1 (0.3)	0.0 (0.0)	n.d.	n.d.	-11.1 (0.8)	-11.8 (0.4)

¹n.d. = not determined

Table 4.3: Methane production rates, $\delta^{13}C_{CH_4}$ values, and $\delta^{13}C_{CO_2}$ values for killed control and $^{13}CH_4$ + killed control incubation vials. Error estimates, in parenthesis, are reported as standard deviations of triplicate samples or half of the range of duplicate samples. The bolded values are statistically different, p values < 0.05 , from unamended controls.

		Killed Controls					
		Methane Production Rates (nmol g ⁻¹ d ⁻¹)		$\delta^{13}C_{CH_4}$ Values (‰)		$\delta^{13}C_{CO_2}$ Values (‰)	
Sample Site		Killed Controls	Killed Control + ¹³ CH ₄	Killed Controls	Killed Control + ¹³ CH ₄	Killed Controls	Killed Control + ¹³ CH ₄
Atacama Desert (2013)	LL2	0.0 (0.0)	n.d.	n.d.	n.d.	n.d.	n.d.
	LL3	0.0 (0.0)	n.d.	n.d.	n.d.	n.d.	n.d.
	LL4	0.0 (0.0)	n.d.	n.d.	n.d.	n.d.	n.d.
	LL8	0.0 (0.0)	n.d.	n.d.	n.d.	n.d.	n.d.
	Cejar 1	-0.1 (0.1)	n.d.	n.d.	n.d.	n.d.	n.d.
	Cejar 2	0.5 (0.2)	n.d.	n.d.	n.d.	n.d.	n.d.
	Cejar 3	0.0 (0.0)	n.d.	n.d.	n.d.	n.d.	n.d.
	CX1	-0.2 (0.7)	n.d.	n.d.	n.d.	n.d.	n.d.
	ET2	77.1 (1.1)	n.d.	-74.8 (0.1)	n.d.	-5.9 (0.2)	n.d.
Baja (2012)	1	n.d. ¹	n.d.	n.d.	n.d.	n.d.	n.d.
	1-Deep	n.d.	n.d.	n.d.	n.d.	n.d.	n.d.
	9	n.d.	n.d.	n.d.	n.d.	n.d.	n.d.
	10	0.0 (0.0)	n.d.	n.d.	n.d.	n.d.	n.d.
	10-Deep	0.0 (0.0)	n.d.	n.d.	n.d.	n.d.	n.d.
Baja (2014)	1	0.2 (0.1)	0.1 (0.3)	n.d.	n.d.	-11.2 (0.6)	-11.1 (0.8)
	9	0.0 (0.0)	0.0 (0.0)	n.d.	n.d.	-11.7 (0.8)	-11.8 (0.4)

¹n.d. = not determined

Table 4.4: The $\delta^{13}\text{C}_{\text{POC}}$ values and particulate organic carbon (POC) concentrations for Guerrero Negro, Baja California Sur, Mexico, and Atacama Desert, Chile sites. The $\delta^{13}\text{C}_{\text{DIC}}$ values and dissolved inorganic carbon (DIC) concentrations are from site water collected at each field site. Error estimates are in parenthesis and reported as standard deviations of triplicate samples or half of the range of duplicate samples

Sample Site		$\delta^{13}\text{C}_{\text{POC}}$ Values (‰)	POC (%)	$\delta^{13}\text{C}_{\text{DIC}}$ Values (‰)	DIC (mM)
Atacama Desert (2013)	LL2	-12.1 (0.2)	0.3 (0.03)	4.4 (0.9)	1.1 (0.2)
	LL3	-12.2 (0.1)	0.2 (0.03)	4.8 (0.8)	1.1 (0.0)
	LL4	-8.9 (0.1)	1.7 (0.04)	2.6 (2.3)	1.2 (0.0)
	LL8	-10.8 (0.0)	2.5 (0.42)	-1.9 (0.4)	0.6 (0.2)
	Cejar 1	-9.7 (0.5)	6.3 (1.21)	-1.3 (1.2)	3.9 (1.1)
	Cejar 2	-11.0 (0.2)	2.0 (0.30)	-2.2 (1.3)	4.2 (0.2)
	Cejar 3	-13.0 (0.2)	0.1 (0.01)	0.2 (0.1)	3.8 (0.5)
	CX1	-5.5 (0.2)	3.6 (0.32)	8.7 (0.9)	1.1 (0.3)
	ET2	-14.5 (0.0)	4.5 (0.08)	-5.4 (0.4)	1.7 (0.3)
Baja (2012)	1	-9.7 (0.2)	10.1 (0.46)	n.d. ¹	n.d.
	1-Deep	-10.7 (0.2)	9.4 (0.32)	n.d.	n.d.
	9	-14.7 (0.2)	0.2 (0.00)	n.d.	n.d.
	10	-17.2 (1.8)	0.1 (0.01)	n.d.	n.d.
	10-Deep	-5.4 (2.6)	0.7 (0.10)	n.d.	n.d.
Baja (2014)	1	-9.8 (0.0)	12.1 (0.39)	1.9 (0.4)	2.4 (0.1)
	9	-12.8 (0.3)	0.2 (0.01)	-1.4 (0.0)	2.0 (0.1)

¹n.d. = not determined

Table 4.5: Dissolved inorganic carbon (DIC) concentrations, $\delta^{13}\text{C}_{\text{DIC}}$ values, and DIC production rates for all Guerrero Negro, Baja 2014 incubations. Error estimates are in parenthesis and reported as standard deviations of triplicate samples or half of the range of duplicate samples, except when error was propagated (denoted by an asterisk). Propagated error was reported in place of standard deviations or half ranges only when the calculated error was larger than standard deviations or half ranges. The bolded and italicized values are statistically different, p values < 0.05 , from unamended controls, while the bolded $^{13}\text{CH}_4$ +inhibitor values are statistically different from their corresponding inhibitor treatment (i.e., $^{13}\text{CH}_4$ +BES vs. BES).

Guerrero Negro, Baja (2014)							
Incubation Samples	DIC (mM)		$\delta^{13}\text{C}_{\text{DIC}}$ Values (‰)		DIC Production Rates (nmol g ⁻¹ d ⁻¹)		
Controls	Area 1	Area 9	Area 1	Area 9	Area 1	Area 9	
Anaerobic Control	14.7 (2.1)*	3.5 (0.7)	-3.0 (1.1)	-3.2 (0.2)	5298.5 (1529.8)	74.7 (29.0)	
Aerobic Control	15.6 (2.4)*	7.0 (0.8)	-4.5 (0.4)	-4.8 (0.5)	5435.8 (1367.3)	113.4 (12.9)	
Amended Treatments							
Anaerobic	BES	17.0 (3.1)*	2.9 (0.7)	-3.8 (0.1)	<i>-1.4 (0.3)</i>	6227.0 (35.0)	44.0 (30.0)
	Molybdate	11.8 (1.6)*	<i>1.7 (0.4)</i>	-0.9 (0.9)	-2.8 (0.7)	3891.2 (501.3)	<i>-13.1 (17.8)</i>
	$^{13}\text{CH}_4$	16.0 (2.6)*	3.4 (0.4)	-3.3 (0.4)	<i>-1.1 (0.5)</i>	5635.3 (101.8)	-17.2 (68.5)
	$^{13}\text{CH}_4$ + BES	14.5 (2.5)*	3.6 (0.3)*	-3.1 (0.3)	-1.5 (1.4)	<i>4524.1 (272.0)</i>	76.8 (6.4)
	$^{13}\text{CH}_4$ + Molybdate	13.5 (1.9)*	1.2 (0.1)	-0.8 (0.5)	-1.4 (0.3)	4582.1 (1142.2)	-32.6 (4.1)
Aerobic	BES	15.6 (2.5)*	5.9 (0.6)*	-3.5 (0.4)	-5.2 (0.6)	5404.7 (820.5)	94.3 (3.3)
	Picolinic Acid	16.7 (2.5)*	5.7 (0.4)*	-3.5 (1.4)	-5.1 (0.2)	5429.4 (311.1)	97.6 (4.5)
	Killed Control	16.2 (2.4)*	<i>2.2 (0.2)</i>	-3.8 (0.4)	<i>-2.0 (0.0)</i>	5697.5 (96.7)	<i>6.3 (5.4)</i>
	$^{13}\text{CH}_4$	19.0 (2.5)*	7.8 (0.7)	-3.6 (0.2)	-4.9 (0.4)	6544.0 (190.3)	135.1 (16.2)
	$^{13}\text{CH}_4$ + BES	17.3 (2.6)*	6.9 (1.1)	-3.3 (0.7)	-4.7 (0.0)	5931.7 (699.5)	116.5 (24.4)
	$^{13}\text{CH}_4$ + Picolinic Acid	18.8 (2.7)*	7.3 (0.6)	-3.8 (0.4)	-4.1 (0.4)	6749.6 (791.5)	128.4 (14.2)
	$^{13}\text{CH}_4$ + Killed Control	16.1 (2.1)*	2.0 (0.0)	-3.7 (0.2)	<i>-0.8 (0.1)</i>	5454.7 (191.4)	0.5 (1.1)

* = propagated error

Table 4.6: Anion concentrations of chloride (Cl^-) and sulfate (SO_4^{2-}) for water samples from Guerrero Negro, Baja California Sur, Mexico and the Atacama Desert, Chile sites. Reported next to approximate concentrations for seawater. Error estimates are in parenthesis and reported as standard deviations of triplicate samples or half of the range of duplicate samples.

Sampling Sites		Cl^- (mM)	SO_4^{2-} (mM)
Seawater		560	29
Atacama Desert (2013)	LL2	1795.1 (48.7)	154.1 (18.6)
	LL3	1839.2 (6.7)	231.8 (17.8)
	LL4	2101.1 (105.2)	200.5 (14.2)
	LL8	835.7 (79.2)	161.1 (16.1)
	Cejar 1	724.2 (139.2)	88.3 (9.6)
	Cejar 2	698.4 (105.2)	101.9 (12.1)
	Cejar 3	829.9 (59.1)	115.5 (3.5)
	CX1	1394.3 (45.3)	110.9 (0.5)
	ET2	127.7 (43.9)	1.8 (0.4)
Baja (2012)	1	1065.1 (19.3)	39.3 (2.0)
	9	2973.0 (66.9)	126.5 (1.3)
	10	5458.4 (194.5)	188.7 (3.0)
Baja (2014)	1	1079.1 (153.1)	55.38 (0.7)
	9	2562.9 (144.1)	130.3 (0.1)

Table 4.7: The $\delta^{13}\text{C}_{\text{CO}_2}$ values for unamended control and $^{13}\text{CH}_4$ -amended incubations, $\delta^{13}\text{C}_{\text{DIC}}$ values for sites showing enrichment in $\delta^{13}\text{C}_{\text{CO}_2}$ values between unamended anaerobic controls and $^{13}\text{CH}_4$ -amended incubations. Expected $\delta^{13}\text{C}_{\text{CO}_2}$ values are based on the estimated atom% of CH_4 in $^{13}\text{CH}_4$ -amended incubations, and estimated DIC production rates determined from Area 1 and 9 (Baja 2014) measurements. An estimated and relatively conservative methane oxidation rate of $0.05 \text{ nmol g}^{-1} \text{ d}^{-1}$, based on previously published studies of hypersaline lakes by Iversen et al., 1987, and Joye et al., 1999, was used to calculate expected $\delta^{13}\text{C}_{\text{CO}_2}$ values. Error estimates are in parenthesis and reported as standard deviations of triplicate samples or half of the range of duplicate samples.

Atacama Desert (2013)		
Sampling Sites	LL 2	LL 4
	Anaerobic	Anaerobic
Measured Values		
$\delta^{13}\text{C}_{\text{CO}_2}$ Values (‰) Unamended Control Incubations	- 11.7 (0.3)	- 21.7 (0.3)
$\delta^{13}\text{C}_{\text{CO}_2}$ Values (‰) $^{13}\text{CH}_4$ -amended Incubations	- 8.0 (1.4)	- 15.0 (0.1)
Measured Enrichment in $\delta^{13}\text{C}_{\text{CO}_2}$ Values (‰)	+ 3.7	+ 6.7
Measured $\delta^{13}\text{C}_{\text{DIC}}$ Values (‰)	+ 4.4 (0.9)	+ 2.6 (2.3)
Calculated Values		
Estimated DIC Production Rate ($\text{nmol g}^{-1} \text{ d}^{-1}$)	75	900
Estimated CH_4 atom% in $^{13}\text{CH}_4$ -amended Incubations	66	90
Expected $\delta^{13}\text{C}_{\text{CO}_2}$ Values (‰)	+ 35	- 1
Approximate Methane Oxidation Rates ($\text{nmol g}^{-1} \text{ d}^{-1}$)	< 0.0001	< 0.0001

9. FIGURES

Figure 2.1: Global locations of study sites Guerrero Negro, Baja California Sur, Mexico and the Atacama Desert, Chile. (Photo property of Google Earth.)



Figure 2.2: Guerrero Negro, Baja California Sur, Mexico sampling locations. Area numbers increase with increasing salinity. (Photo property of Google Earth.)

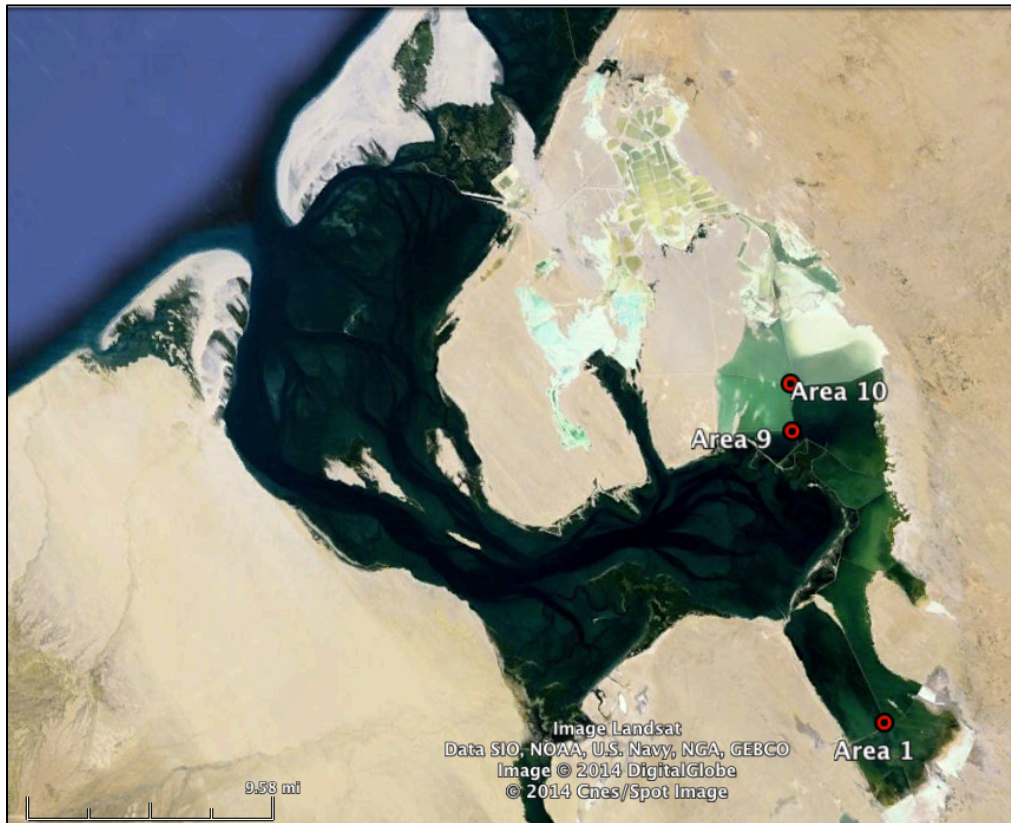


Figure 2.3: The Atacama Desert, Chile sampling location. Areas include four sites in Salar de Llamara, four in Salar de Atacama, and one site in the El Tatio geyser field. (Photo property of Google Earth.)



Figure 2.4: Gypsum head from Area 9 of Guerrero Negro, Baja California Sur, Mexico. Colorful laminations of greens and reds distinguish between the different endoevaporite microbial communities. (Photo courtesy of Angela Detweiler.)



Figure 2.5: The Atacama Desert, Chile sampling locations. Four site locations at Salar de Llamara (LL 2, 3, 4 and 8), and three at Laguna Cejar (Cejar 1, 2, and 3). (Photo property of Google Earth.)



Figure 2.6: The Atacama Desert, Chile sampling locations. One site location at Laguna Chaxa (CX 1) and one at the El Tatio geyser field. (Photo property of Google Earth.)



Figure 4.1: Methane production rates for unamended anaerobic and aerobic control incubations vials, and $^{13}\text{CH}_4$ -amended incubation vials. Areas denoted with an asterisk (*) represent Guerrero Negro, Baja 2014 samples.

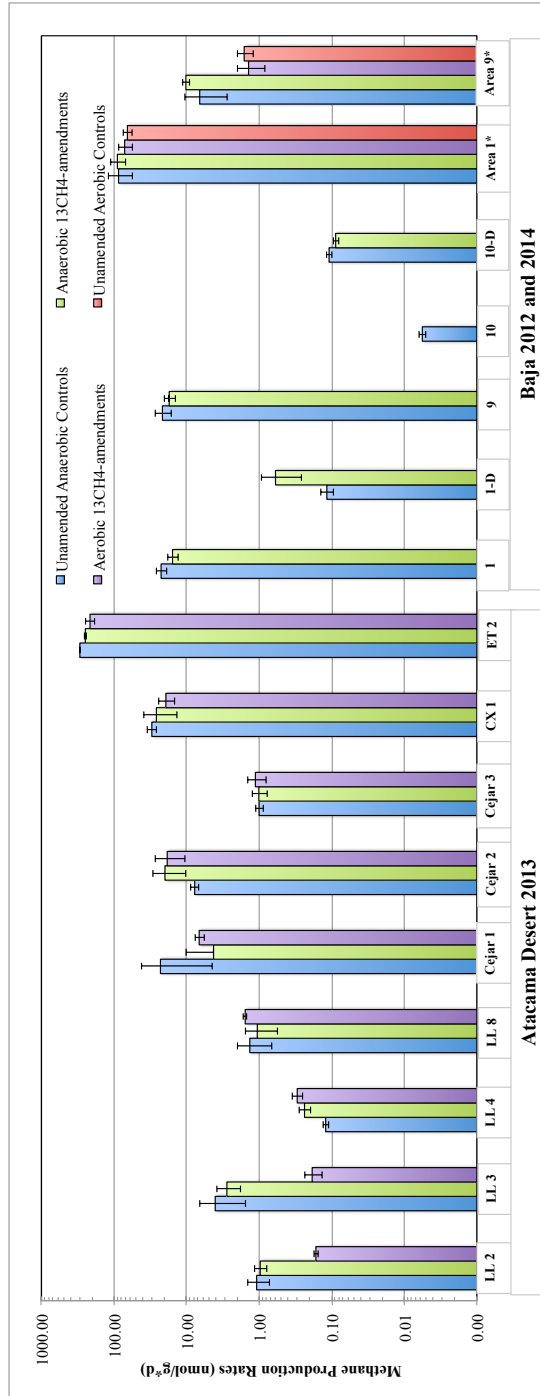


Figure 4.2: The methane production rates for unamended controls, inhibitor, and $^{13}\text{CH}_4$ +inhibitor incubation experiments of Area 1 and Area 9 from Baja (2014). The inhibitor treatments were compared to unamended controls, while the $^{13}\text{CH}_4$ +inhibitor treatments were compared to their corresponding inhibitor alone treatments (i.e., $^{13}\text{CH}_4$ +BES vs. BES).

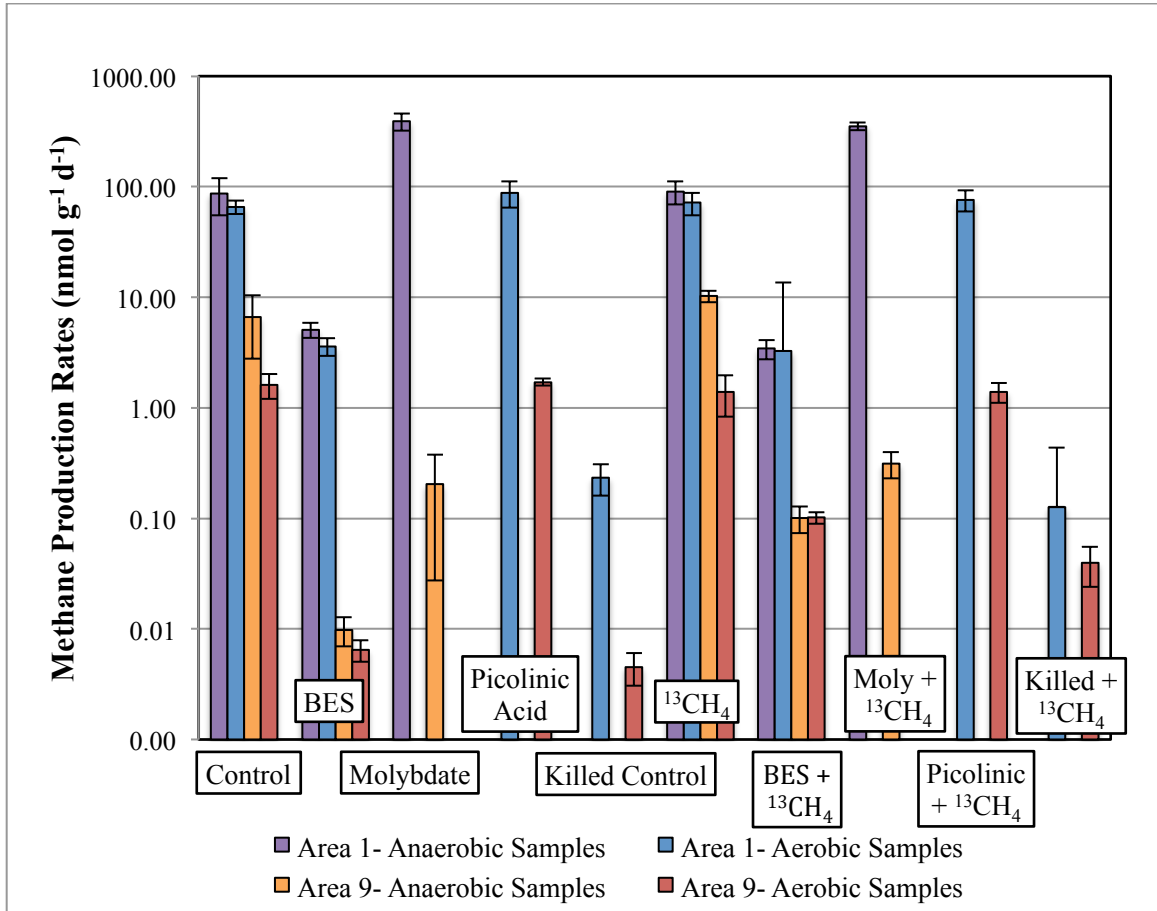


Figure 4.3: The $\delta^{13}C_{CH_4}$ values for unamended anaerobic and aerobic control incubations vials. Areas denoted with an asterisk (*) represent Baja 2014 incubations.

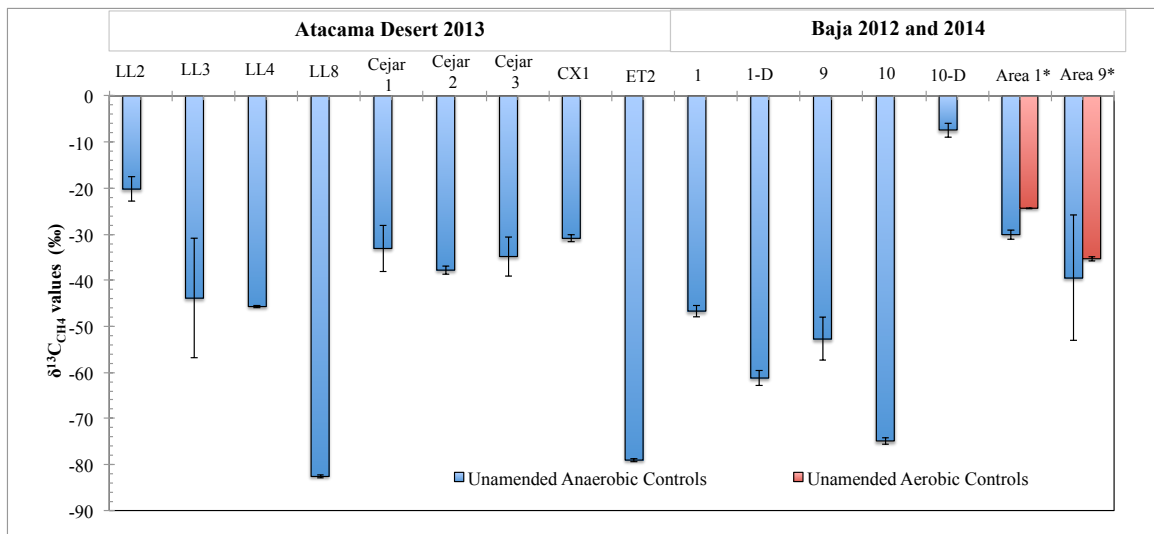


Figure 4.4: The $\delta^{13}\text{C}_{\text{CO}_2}$ values from unamended controls and $^{13}\text{CH}_4$ -amended incubation vials of Baja (2012 and 2014) and Atacama Desert (2013) sites. Areas denoted with an asterisk (*) represent Baja 2014 samples. Since aerobic controls were not prepared for the Atacama Desert 2013 study, aerobic $^{13}\text{CH}_4$ -amended incubations for Atacama Desert 2013 were compared to anaerobic controls.

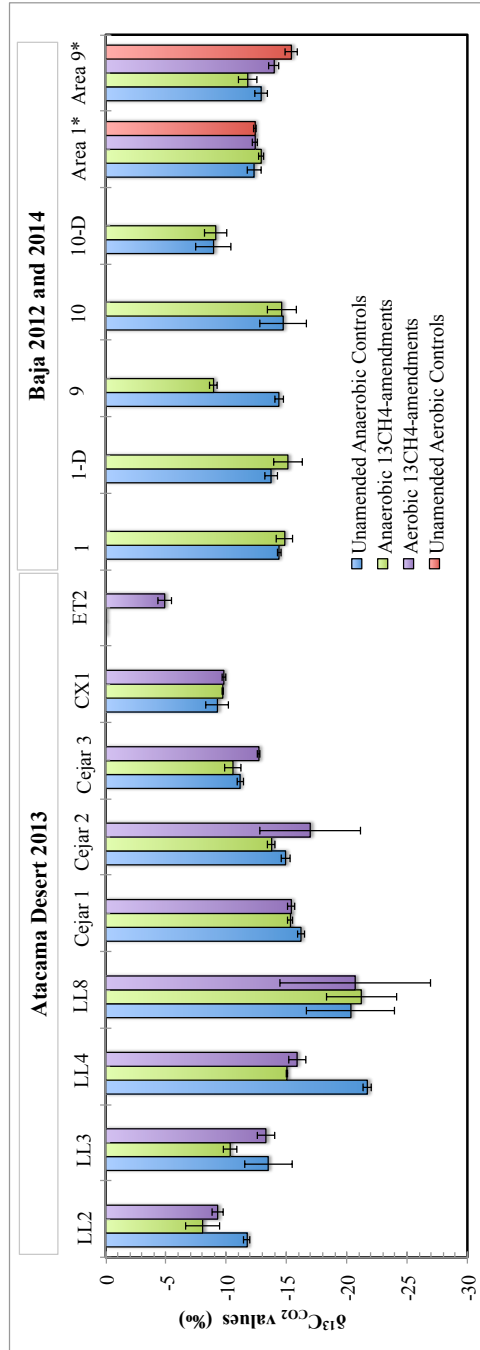


Figure 4.5: The $\delta^{13}\text{C}_{\text{CO}_2}$ values for unamended controls, inhibitor, and $^{13}\text{CH}_4$ +inhibitor incubation experiments of Area 1 and Area 9 from Baja (2014). The inhibitor treatments were compared to unamended controls, while the $^{13}\text{CH}_4$ +inhibitor treatments were compared to their corresponding inhibitor alone treatments (i.e., $^{13}\text{CH}_4$ +BES vs. BES).

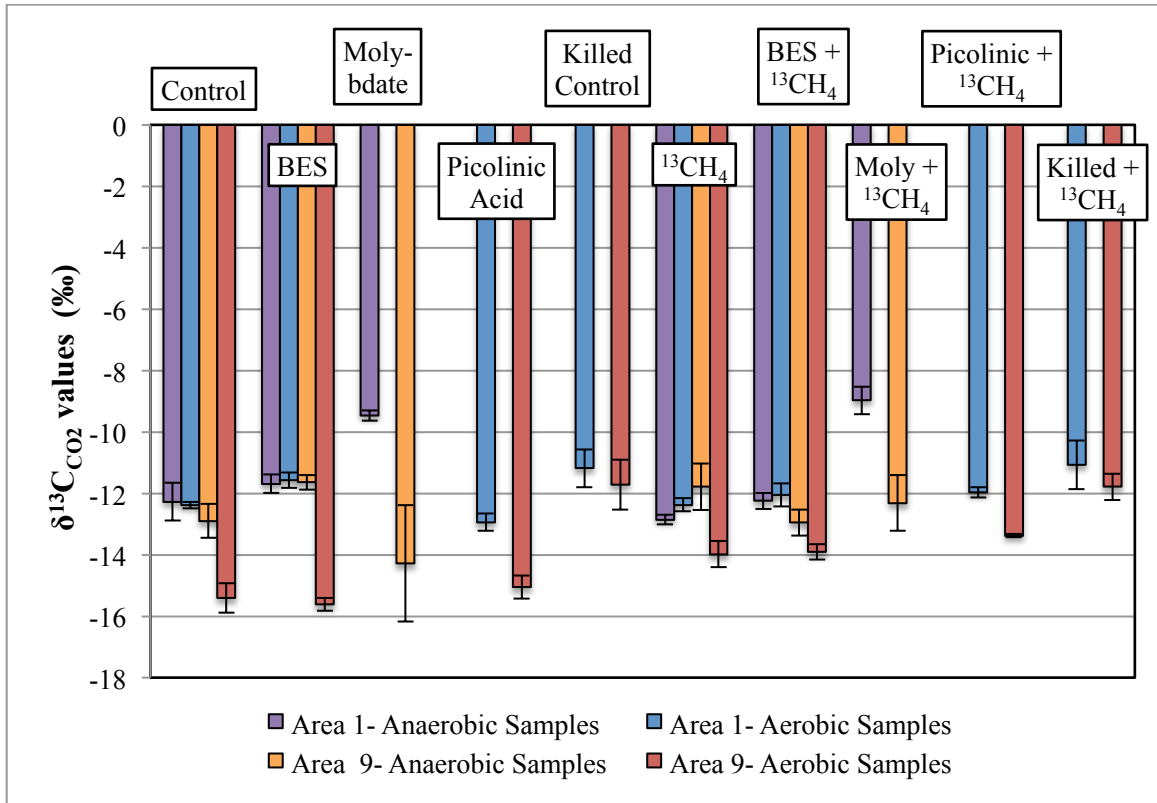


Figure 4.6: Averaged POC concentrations from Guerrero Negro, Baja California Sur, Mexico, and the Atacama Desert, Chile sites compared to salinity. Areas denoted with an asterisk (*), represent Baja 2014 samples.

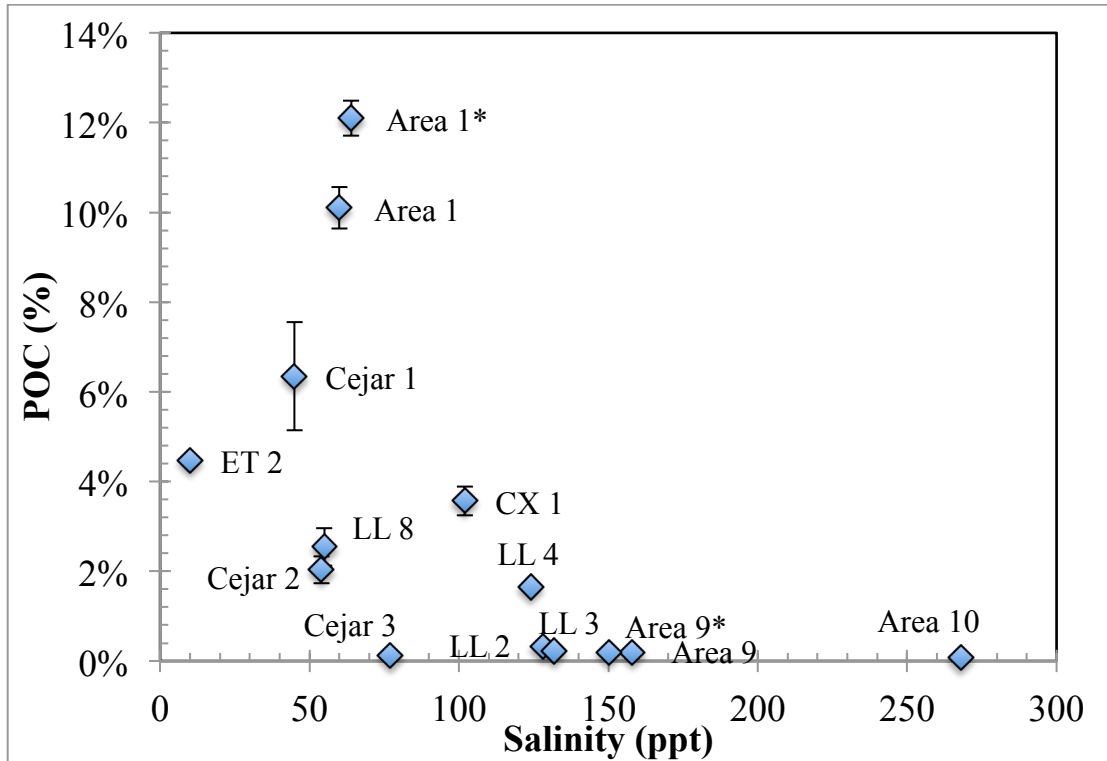


Figure 4.7: Averaged chloride concentrations (Cl^-) as a function of salinity for water samples collected from Guerrero Negro, Baja California Sur, Mexico, and the Atacama Desert, Chile sites. For reference, estimated chloride concentrations of seawater are plotted (using a chloride seawater value of 560 mM). Areas denoted with an asterisk (*), represent Baja 2014 samples.

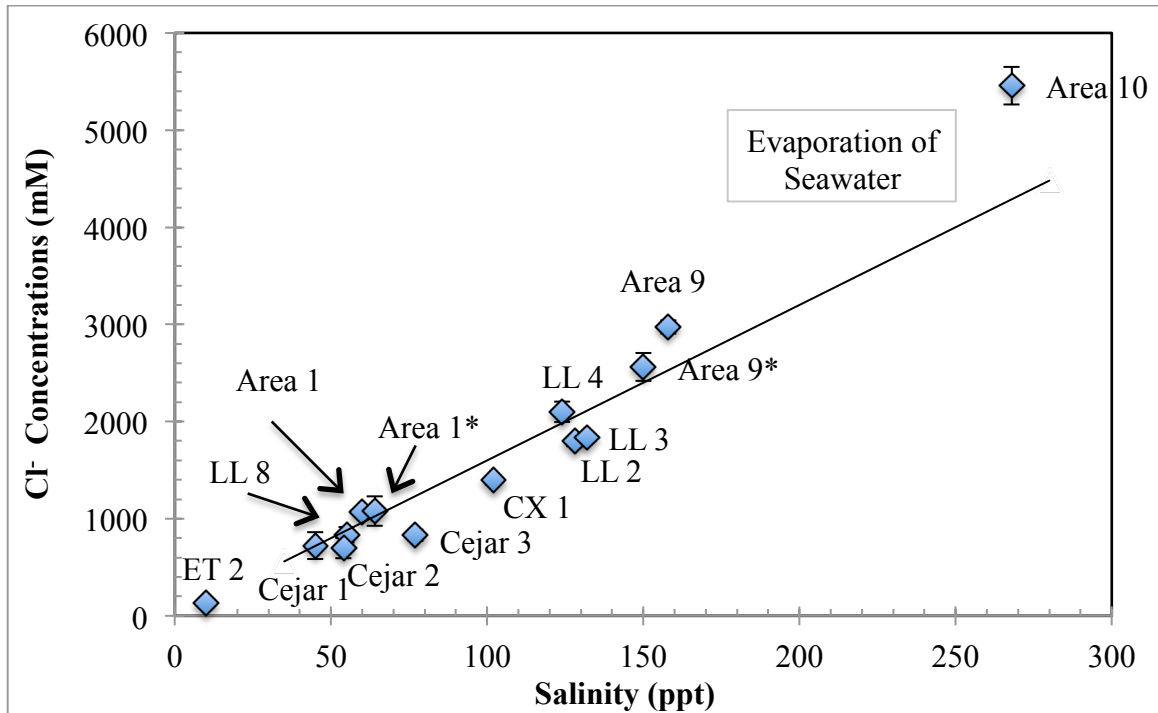


Figure 4.8: Averaged sulfate (SO_4^{2-}) as a function of salinity for water samples collected from Guerrero Negro, Baja California Sur, Mexico, and the Atacama Desert, Chile sites. For reference, estimated sulfate concentrations of seawater are plotted (using a sulfate seawater value of 29 mM). Areas denoted with an asterisk (*), represent Baja 2014 samples.

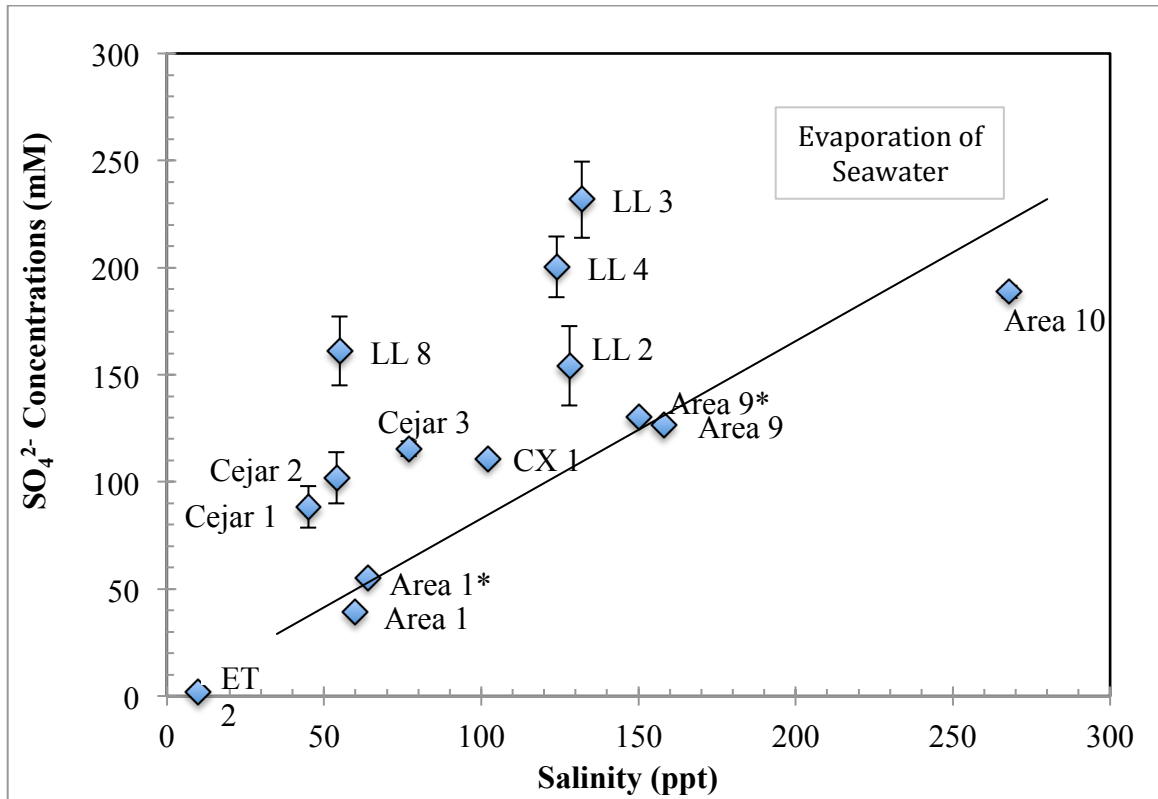


Figure 5.1: Methane production rates versus concentrations of particulate organic carbon (POC) for all sample sites in Guerrero Negro, Baja California Sur, Mexico, and the Atacama Desert, Chile. Shows methane production rates increase with POC concentrations.

